INTERNATIONAL
HELLENIC
UNIVERSITY

School of Economics & Business Administration

MSc Strategic Product Design

Dissertation Title:

The effect of k-wire diameter, pretension and material to the rigidity of Ilizarov external bone fixator

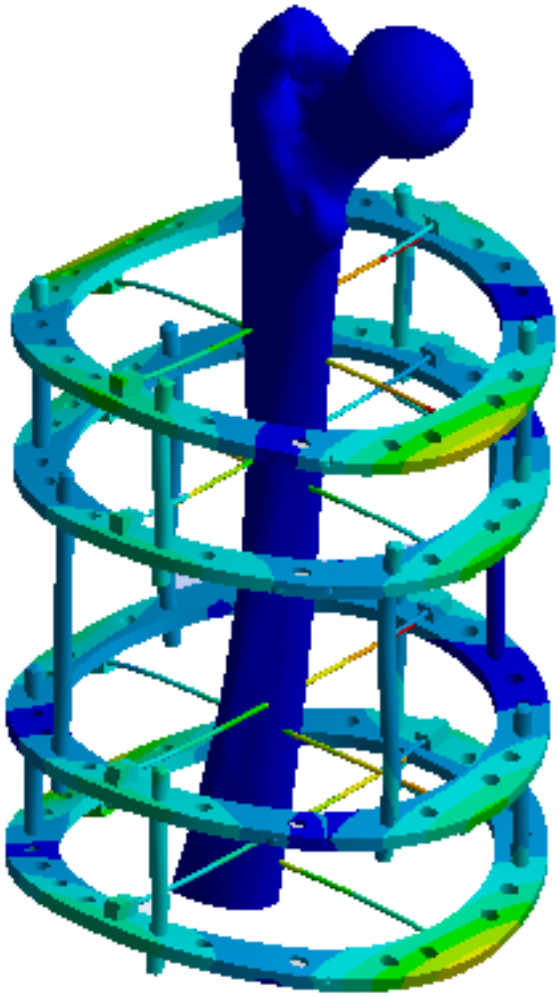

Grigoriadis Nikolaos

Thessaloniki 2014

Abstract

The mechanical behavior of the parts of the Ilizarov external bone fixator, such as the steel rings and the kirschner wires, plays a defining factor in the overall stiffness, stability, and reliability of an external fixation system. The objective of the present study is the construction of a reliable numerical model of the standard Ilizarov fixator comprised of metallic and composite biocompatible materials, allowing for a detailed parametric investigation of various factors influencing the effectiveness of the technique. Such factors are considered to be the axial and bending stiffness. In the present study, the impact of changing the Kirschner wires' (k-wires) diameter and pretension to the overall fixator stiffness, will be investigated assuming that the diameter of the rings and the angle between the wires is constant. Furthermore, the bone fixator interface is going to be studied by considering only the k-wires' pretension, as well as both the k-wires pretension and dead load weight bearing. Three different Ilizarov variations are going to be investigated, the standard Ilizarov frame manufactured by 316 stainless steel, a Titanium alloy and finally a fixator completely made by composite materials, i.e. carbon fiber Polyether ether ketone (CF/PEEK).

Acknowledgements

Firstly, I would like to thank the International Hellenic University for giving be the opportunity, the knowledge and means to deal with such an interesting scientific field as biomechanics is.

Secondly, I would like to thank Professor Nikolaos Michailidis whose help and guidance was critical through the whole research process. His extensive knowledge of biomechanics, materials and finite element techniques was crucial factor for the completion of the current study.

Special thanks I owe to Dr. Dimitrios Tzetzis who guided and encouraged me through my whole MSc studies. His academic experience appeared to be helpful also for this study. His ideas during this dissertation proved to be salutary to overcome difficult problems that occurred though out this process.

Furthermore, I would like to thank Dr. Alexandros Tsouknidas for his contribution on the 3D modeling of the femur bone. Modeling of tissues is a time consuming and difficult task that demands exceptional skills.

Finally, I would like to thank Mr. Theodoros Fillipou, for his help in understanding the whole Osteogenesis procedure using the Ilizarov external fixator. His descriptions and experience of the applied fixator on a third degree fracture, and his experience living with it, was determinant for the complete understanding of the postoperative process.

Last but not least I would like to thank my family for their continuous support during my studies and my professional carrier.

Table of Contents

1. Introduction 6

1.1. General Overview 6

1.2. Purpose 6

1.3. Objective 7

1.4 Structure 8

2. Literature Review 9

2.1 Medical Review 9

2.2 Ilixarov External Bone Fixator 12

2.3 Ilizarov Design 18

2.4 Biocompatible Materials 20

3. Methodology 22

3.1 Methodology Review 22

3.2 3D Modeling 23

3.3 FEM Modeling 26

3.4 Material Modeling 28

3.5 Model of Load and Boundary Conditions 29

3.6 Model Convergence 29

4. Results and Discussion 30

4.1 Deformation of the System 30

4.2 Comparative Results 36

5.Conclusions Suggestions 50

6. Future Work 51

References 52

1. Introduction

1.1 General overview

An initial literature overview is going to take place in the following chapters in order to understand bone's physiology. Fractures and osteogenesis will be described in medical terms. Prior to the detailed description of the Ilizarov surgical process, the framework under which those fractures occur and the natural healing process will be presented. The Ilizarov external bone fixator will be presented and analyzed with respect to the different parts and the possible assembly configurations. Such an analysis will help to the better understanding of the application. Finally, a detailed design analysis of the apparatus will take place in order for the critical factors that affect the healing process to be pointed out.

A short review of biocompatible materials will be also presented, regarding their properties and their range of application.

For the conduction of the present study, the geometrical aspects of the Ilizarov external bone fixator will be designed in Solidworks according to the literature. A finite element model will be developed in the Ansys software and the boundary conditions that describe the problem will be set. The external loads are going to be applied on the FEA model and the results are going to be presented and discussed.

Two different variations of 180 mm ring Ilizarov external fixator will be studied. The first one will be attached to a femur bone with 1.8 mm thick wires, while for the second one 2 mm thick k-wires will be used. These two variations are going to be studied on two different load states and they are going to be loaded with five different k-wire pretension loads. Three different materials are going to be studied concerning their performance with respect to the bone-fixator interface.

1.2 Purpose

There are several anatomical, orthopedic, and mechanical critical factors affecting the outcome of treatment, using the Ilizarov technique. The purpose of this biomechanical study of the Ilizarov external bone fixator is to analyze the mechanical factors, like material and mechanical loads on the frame in order to observe and record their interaction with the human bone. Such an investigation will give an insight of the bone-fixator interface and it will highlight the importance of the optimal combination

of adjustments serving for the healing process, along with the preoperative Ilizarov modules selection for the achievement of the stiffer possible assembly.

1.3 Objective

Ilizarov external bone fixator is a modular apparatus consisted of external rings fixed on the fractured bone employing thin kirchner wires (k-wires). These thin wires have are tensioned, and by taking advantage of the stress stiffening effect that occurs they offer a stable and yet dynamic environment for the fracture healing process. The hypothesis behind the studied problem lies on the fact that wire tension combined with ring's stiffness is critical for the wire-bone interface and the healing process. The impact of this combination have been studied by Gessmann (2011) that has shown the substantial influence of bearing load on the biomechanical characteristics of the apparatus. Mullins (2003) and Osei (2006) both tested the clamps-wire interface in order to study wire slippage versus clamp's pretension relationship. Different wire holding methods were tested by Davidson (2003), La Russa (2011) and Gessmann (2012) in order to maintain the k-wire pretension. Residual wire tension after dynamic loading has been studied by Renard (2005) concluding on severe pretension loss after the first loading cycles. The impact of wire tension versus frequency studied by La Russa (2010) by performing an acoustic analysis on 20 k-wires both deformed and non-deformed in an effort to develop a mathematical model to investigate the effect of k-wire pretension and frame construction on wire tension.

The importance of finite element analysis in biomechanics problems was pointed out by Prendergast (1997). Since then several mathematical models have been developed with the use of finite elements software, allowing the prediction of deformations in musculoskeletal structures, exploring the mechanical basis of fracture healing bone remodeling. Mrazek (2010) compared the physiological state of tibia before and after the application of an external fixator. For this study he used two different types of fixators and compared the deformations of healthy bone to those of the bone with applied external fixator in three different load states. The results are indicating that the displacements of the healthy bone are smaller than in both cases of fixation. Georgadakis (2010) developed a finite element model to investigate the axial displacement of the Ilizarov external bone fixator. In this study, he used rings having a diameter of 150 and 180 mm , with 1.5, 1.8 and 2 mm thick k-wires, tensioned in five different levels. Zamani (2010) developed also a theoretical and a computational

model comparing the results. Those results appeared to converge, assuring the reliability of such finite element models.

The conducted studies are indicating the importance of k-wires diameter, pretension, clamping, ring diameter, and material on the overall stiffness of Ilizarov apparatus. The influence of the initial k-wire pretension by itself on the bone has not been studied yet. The k-wire pretension load is causing bending on the external rings. The displacement of the ring is therefore loading the bone even prior the dead weight bearing load. This interaction is going to be studied during the k-wires pretension load only and the equivalent load that occurs after the dead weight loading.

1.4 Structure

Chapter 2 describes the literature review and more specifically the medical overview, where the physiology of human body is presented along with the bones morphology. The constitution of bones is also described in this chapter, with respect to the different layers and their contribution to physical processes taking place during fracture healing. Ilizarov's mechanism history is presented, highlighting the sociopolitical conditions which lead to the apparatus development. A step by step description of the surgical application of the fixator is following, pointing out the difficulties and key points of the procedure. A detailed description of the Ilizarov modular fixator is following with respect to the different parts consisting it and the function of these parts. The Ilizarov apparatus is disassembled and the several modulus are presented conducting a separate design analysis for each part. By this analysis the advantages and drawbacks of the procedure are highlighted. The mechanics of the apparatus is described identifying the critical factors like the material, the dimensions of the different modules and the mechanical loads, affecting the Ilizarov bone fixator stability and rigidity. Finally, a short description of biocompatible materials is following in order to explain their properties and highlight their advantages, drawbacks and range of application.

In the third chapter, a methodology overview is presented after the identification of the problem and a detailed description of the different steps is taking place. The 3D modeling procedure and techniques, necessary for the solution are described. Furthermore, the FEM modeling procedure is presented with respect to the sequential steps followed, explaining the meshing techniques, showing the boundary conditions and load application areas have been used, to solve the studied problem.

In the fourth chapter, the results of the conducted study are presented and explained. The presentation of these results will be done with the use of figures (graphical representation), tables and charts. With the use of these tables and charts the comparative presentation will be possible and the results will be further discussed.

After the discussion in chapter 4, the fifth chapter will describe the future work which will take place using the extracted results.

Finally, in the sixth chapter conclusions and suggestions of the present study outcomes will be presented, summarizing the work that have been done during this research.

2. Literature review

2.1 Medical Overview

People nowadays are trying more often to overcome their limits doing extreme sports and activities. This often leads to accidents and complicated injuries including also fractures. In particular, two basic types of fractures can be distinguished, the simple and the complicated one.

There is no life threat in case of simple fractures. The treatment is based on adjustment of fractures and their fixation. These fractures are mostly cured using plaster bandage. The treatment of complicated fractures is much more difficult. Bone tissue, as well as soft tissue injuries happens in most cases.

Bones are rigid organs that constitute part of the endoskeleton of human body. They support and protect the various organs which are critical for life support. Bones come in a variety of shapes and have a complex internal and external structure, they are lightweight yet strong and hard, serving multiple functions. Human body consists of 206 separate bones.

Bones structure according to Ralston (2013) consists of several types of tissues, which are responsible for their biological and mechanical behavior shown in Figure 1. The cortical bone is the outer layer of the bone. It is hard with low porosity (5-30%) and it accounts 80% of the total bone mass in a human. It forms an envelope around bone marrow and consists of Cartesian canals. Those systems consist of osteon, extracellular matrix and osteocytes surrounding blood vessels. The interior of the cortical bone is filled with the cancellous bone. It is a spongy formation, consists of a

network of rod elements that make the overall organ lighter and allow room for blood vessels and marrow. The external surface of the bones except the joints area is covered by a membrane called periosteum. Periosteum is the place where neurves are ending making it very sensitive. It is also constituting the area where muscles and tendons are attached.

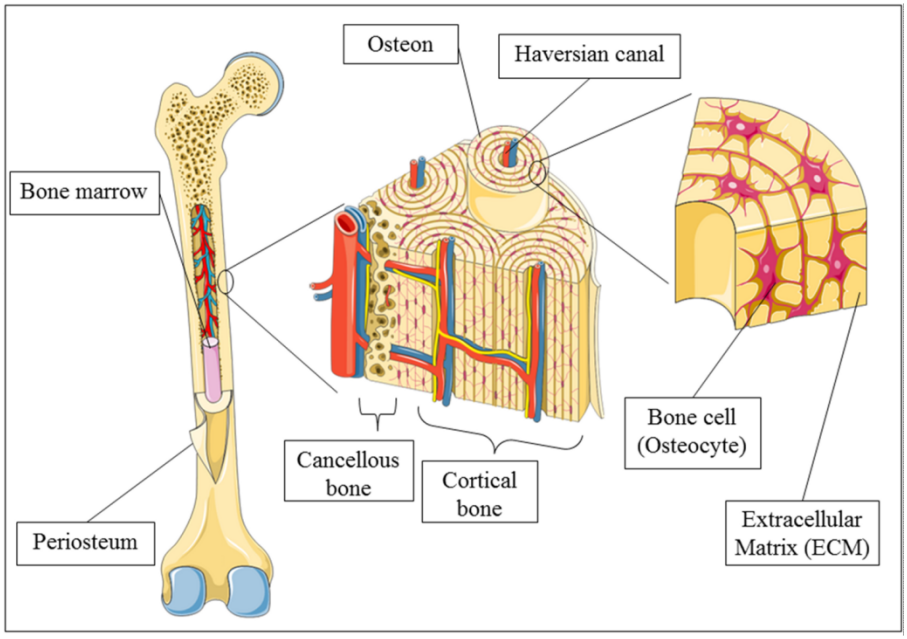

Figure 1 Bone Section view

Bone fracture can be described as a medical condition during which there is a surface continuity interruption. Fractures can be the result of impact, high stresses, or several other medical conditions that weakens the bone, like osteoporosis, bone cancer, or osteogenesis imperfecta. (J.A.Alierta, 2013)

There are several kind of fractures which are classified by the cause their location and orthopedically by their anatomy. Generally traumatic and pathological fractures are referring to the cause of the fracture.

All fractures can be described as closed or open fractures. Closed fractures are those where the soft tissues around them are intact. Open fractures are characterized by open wounds communicating with the fracture area. Several other classifications of fractures exist in order to describe accurately the cause location and morphology. Several factors influence facture healing according to Alierta (2014) such as genetic, cellular and biochemical factors, blood supply, age, the type of fracture and fracture geometry.

Osteotomy on the other hand is a surgical procedure during which the bone is cut to shorten, lengthen, or change its alignment. It is performed to correct birth deformities, or to realign a bone that has healed crookedly after a fracture.

There are two basic types of osteotomy concerning the angular bone deformities, the angular only, and the angulation with translation osteotomy, depending on the morphology of the deformity. (B.Ji, 2010)

Corticotomy is a surgical procedure of cutting the bone in two pieces. The main difference from osteotomy is that the two segments are not always splitting. Corticotomy involves only cortex and therefore leaves vessels and periosteum intact leading this way in shorter healing time.

The natural process of bone fracture or osteotomy healing starts when the bone and the surrounding soft tissues start bleeding. Blood clots start forming in the fragment area and new vessels start shaping in the clots. These new vessels are bringing white blood cells and fibroblasts to the area. The white blood cells are removing gradually all the non-viable materials while the fibroblasts are producing collagen fibers, in order to create a matrix. This collagen matrix is replacing the blood clot. Because of the collagen matrix consistency, the bone fragment areas movement is restricted to a small distance, unless severe force is applied on the fragment. At this stage collagen is starting to repose in the bone, forming the bone matrix. The mineralization of the bone matrix by the calcium hydroxyapatite stiffens it, and by this mineralization the new bone is forming. Callus (healing bone) is sufficiently mineralized within 6 weeks, and it does not have the mechanical properties of healthy bone. The replacement process of the callus by mature lamellar bone can take up to 18 months. (T. Zigman, 2013)

The process of reposing in new bone material by the osteoblasts is called osteogenesis (or ossification). Distraction ossification is an established endogenous tissue engineering technique. This method was established for long bone lengthening. It is based on the gradually distraction of the callus after a low energy corticotomy and the preservation of the soft tissues around the fracture area. It is divided in three stages, the latency, distraction and consolidation. The latency stage stars right after the osteotomy and during this phase the natural process of fracture healing is taking place. Latency stage ends when the active distraction is starting. During distraction phase the collagen monomer is added on the bone matrix, forming this way the new bone. Distraction is achieved by mechanical stimulation, forcing biological responses of the

bone to regenerate. Collagen matrix formation, angiogenesis, mineralization and remodeling of callus are taking place during distraction phase. When the desired bone length is achieved the distraction phase stops and the consolidation begins. During this phase the callus is mineralized and eventually is remodeling to cortical bone. (J.A.Alierta, 2013)

External fixation is a surgical process that is used for bone and soft tissues stabilization. Internal fixation is a surgical process where implants made out of stainless steel, titanium or other biocompatible material are fixed on the fragment area by screws, or thin wires in order to stabilize the bones.

External fixators are used to fixate the fractured bones. Except the fracture healing that is already mentioned they are used to treat limb imperfections, where damaged area must be over bridged. The fixation process has principal influence on the quality of bone concretion.

The Ilizarov apparatus is widely used to treat a variety of birth deformities, open bone fractures, limp lengthening, post traumatic osteomyelitis and infected non-unions. It is assembled by the surgeon for the type of treatment, concerning the dimensions and the shape of the segment to be treated. During it‘s application, a number of variables have to be taken into account.

2.2 lizarov External Bone Fixator

Bone fractures have been happening to humans since the beginning of their existence. The treatment of those fractures was always important and critical for survival. Severe increase of injuries and fractures have been observed during the wars and as a result very important discoveries and innovations occurred during these periods in the field of orthopedics.

As a result of war time in 1951, after the Second World War, with the majority of patients suffering from chronic osteomyelitis with bone deficiencies, such as nonunions and deformities, Dr G. A. Illizarov developed the method still used today that bears his name.

His method was very effective for salvaged limps, preventing amputations and returned completely disabled patients to normal activity. As a result his success spread by word of mouth throughout the Soviet Union. A group of Italian orthopedic

surgeons in 1982 learned of his technique, visited Kurgan, mastered it and subsequently published it in order to be known to the rest of the world.

G.A. Ilizarov's technique was a breakthrough to the knowledge gained until then. Birth deformities, severe fractures, osteomyelitis are some of the aliments that can now be corrected with the use of this technique, resulting an improved life quality of the patients. This improvement resulted from the combination of extensive study and application of the Ilizarov's technique and several others.

Ilizarov appliance is a circular external fixation system, shown in Figure 2, by which bone fragments are stabilized using thin k-wires passing through the bone and fixed to an outer frame of rings and threaded rods. It is a modular fixation system, applied by a surgical process and it can be assembled around the limb in numerous variations

The mechanical characteristics of the frame can be altered by stiffness adjustment. By these adjustments, the ideal rigidity for every stage of the healing process can be achieved creating this way the optimal healing environment.

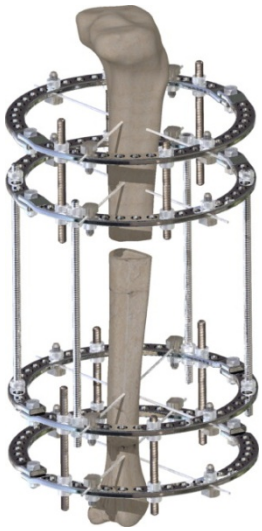

Figure 2 Ilizarov external Bone Fixator

According to Stuard A. Green (1989) chief surgeon of the Rancho Los Amigos Medical Center, who has been visited Kurgan All-Union Scientific Institute to be trained in the Ilizarov's techniques, firstly a percutaneous "corticotomy" is performed rather than an open osteotomy in order to achieve better bone's blood supply. By preserving the bone blood vessels, rapid bone healing is achieved. The Ilizarov bone-cutting procedure is done through a small incision and therefore it does not cause damage to the soft tissues surrounding the bone.

Secondly the k-wires illustrated in Figure 3 are inserted to the patient using a motorized chuck. The k-wires have a square end in order to be driven by the chuck.

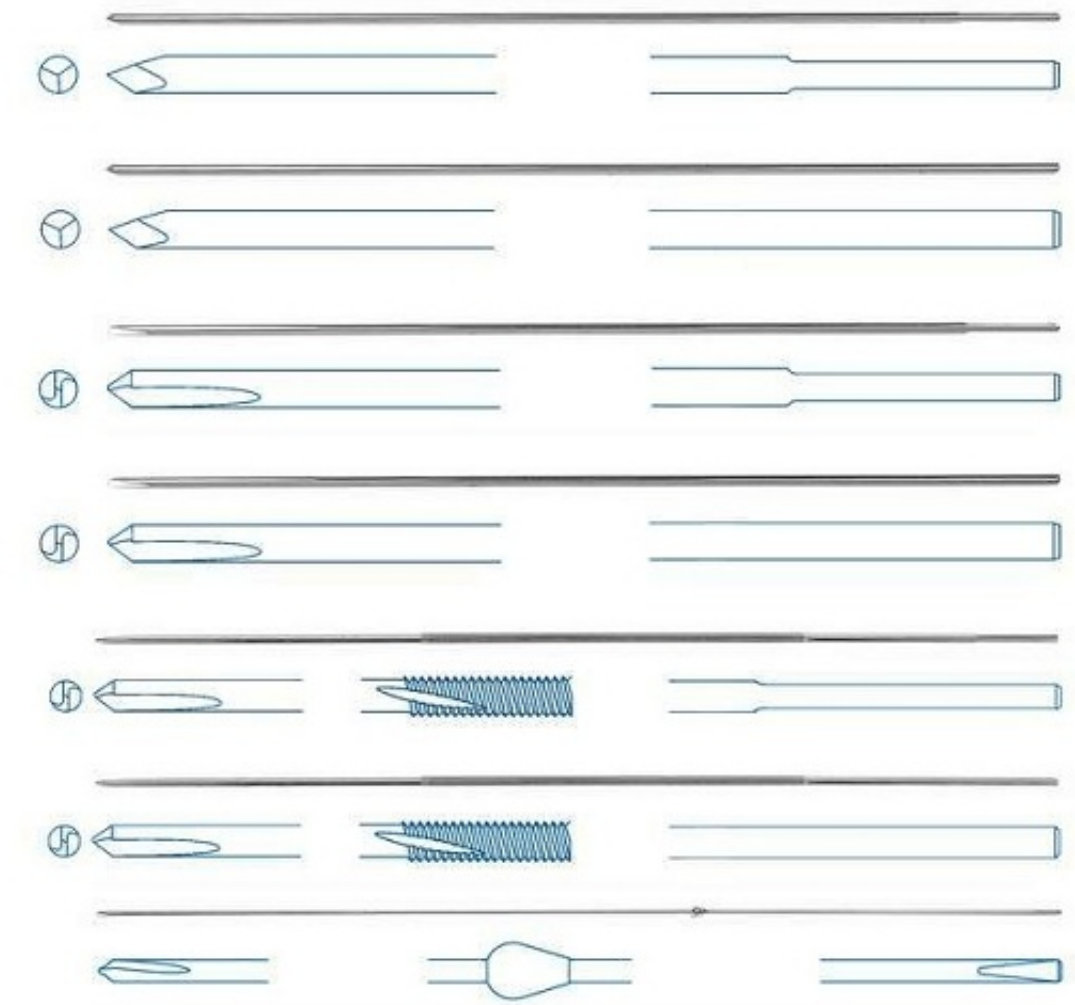

Figure 3 Kirschner wires variations

After the proper placement of the k-wires the assembly of the fixator rings is taking place. The number of rings to be used is essential to achieve the desired rigidity of the assembly. The lower wires are placed in a distance of 20 – 40 mm from the bone fragment.

The k-wires are then attached to the assembled rings. One end of the wire is attached first on the ring assembly with special clamping bolts (Figure 4) and by a dynamometric wire tensioner (Figure 5) it is tensioned to the desired value. The assembly of the second ring follows to the proximal bone with the same process but the stabilization clamping bolt is reversed from the first ring. After the installation of the second ring to the proximal bone the two ring assemblies are attached to each other by hexagonal sockets or threaded rods and their relative position is secured by stainless steel hexagonal nuts.

With the same sequence, the k-wires and rings are attached to the distal bone and their relative position is secured with the same procedure.

The two ring assemblies close to the bone fracture are then connected by hexagonal sockets or threaded rods and stainless steel hexagonal nuts. These connections are very important since the future distraction osteogenesis will occur by the adjustment of these nuts.

Figure 4 k-wire clamp bolts

Figure 5 K-wire tensioner

After the procedure completion, the surgeons are obtaining X-rays to confirm a complete osteotomy and proper wire placement. Seven days after the “corticotomy”, distraction process starts in order to permit preliminary bone healing and early callus formation. During the distraction stage, limps are lengthened by 0.25 mm every six

hours achieving a total elongation of 1 mm per day. This gradual distraction has been proved to be safer and cause less pain to the patients. During the healing process of the bone, regular cleaning of the pin sites is taking place in order to avoid infections.

The real advantage of the Ilizarov apparatus, according to the Catani (2011) study of the Distraction osteogenesis, is that it minimizes angular and rotational movement without affecting the proper elasticity. That appears to be favorable for the bone healing. According to the same study the stability of the assembly is affected by the rigidity of it, the connection to the bone and the stability of the treated segment. Concerning the stability of the apparatus, a critical factor is the material of the half rings. It has to be rigid in order to withstand the equivalent loads from the k-wires tension and bending during the procedure. The diameter of the rings is conversely proportional to the rigidity and therefore the surgeon should choose the smallest possible diameter considering the configuration of the limb. A minimum distance of 2-3 cm between the external ring and the soft tissues is suggested. The number of the rings to be used per bone segment is proportional to the rigidity and therefore it is suggested for the surgeons to use 2 rings per segment.

These two rings on every segment are connected to each other. The type of this connection is critical for the rigidity since it has been observed that hexagonal sockets are far more stable than threaded rods with conical washers. The second type of connection appears to allow angular and rotational movement. In the connection between the two segments conical washers, hinges and universal joints are suggested to be used when angular or rotational adjustments should be done to the frame for the alignment of the bone segments. The number of connections, between the two rings of each segment, is also proportional to rigidity and therefore a minimum number of four connections are necessary.

The diameter, tension, number, and angle between k-wires are also directly proportional to the rigidity of the apparatus. The diameter of the k-wires is usually 1.5 mm for children and 1.8-2.0 mm for adults corresponding to 90 kp maximum tension for 1.5 mm wires and 130 kp for 2 mm wires. The minimum number of k-wires per ring is two and by increasing this number the rigidity of the assembly is increased. The optimal angle between the wires is 90^{o}. Increasing the angle is heightening the stability of the assembly. Because of the intersection of the wires, the maximum angle is 90^{o}, any increment of this value corresponds to smaller supplementary angle.

Furthermore the relative position, between the apparatus and the bone, concerning their longitudinal axis, must be taken into account. The optimal position is difficult to be achieved because of the soft tissue anatomy. The surface area of the bone at the fragment area is very important for the internal stability of the treated segment. It is directly proportional to the rigidity of the apparatus, since larger area corresponds to bigger amount of cancellous bone to restrict movement. Finally, the apparatus rigidity also depends on the maturity of the new bone formation and the amount of soft tissue around it. (M.A. Catagni, 2011)

Summarizing, the parameters that affect the Ilizarov's bone fixator stiffness can be categorized to directly and inversely proportional.

Directly proportional to the rigidity of the assembly are:

- Compressive strength and young's modulus of the ring material
- Number of external rings to be used
- Stability of the rings connection
- The connection elements number
- The diameter of the k-wires
- The number of the k-wires
- Angle between the ring k-wires
- Tension value of the k-wires
- Relevant centralization of the apparatus and the bone
- Fragment surface area
- Maturation of the formed bone

Inversely proportional to the rigidity of the assembly are:

- Length of the rings connection
- Length of the callus formation
- Overall length of the osteogenesis

A very important factor that must been taken into account is the type of the clamping bolt and the pretension of the wire. During treatment, k-wires are under a variable mechanical load which results to k-wire plastic deformation, tension loss or even

fracture. Several studies have indicated a severe tension loss through weight bearing like Renard (2005) and Gessmann (2011). This tension reduction is affecting the bone formation process negatively, increasing the callus formation time. On the other hand bone micro movement appears to be beneficial for the healing process. Therefore, the optimal value of tension versus load should be found.

Another determinant factor for the successful treatment of fractures, using the Ilizarov external bone fixator, is the pin site care. According το Britten (2013) it is a post operational procedure critical to the healthy new bone formation. Several implications have been observed because of insufficient care of the wire sites, like non-unions or the growth of Methicilin Resistant Staphylococcus Aureus (MRSA).

According to Britten (2013), Tyllianakis (2010) and Fenton (2006), pin site defection is varying from 5%-61%. These complications in most of the cases are successfully treated with the use of antibiotics. A small percentage of these complications need hospitalization in order to receive further antibiotic treatment. Only small percentage ends up with a non union. Indicatively, it can be mentioned that from 98 patients that have been treated with the Ilizarov's technique in Leeds Hospital U.K. by Britten (2013) 48 patients developed a pin site infection. Only 3 needed hospitalization, and none of them ended with a non-union. According to Tyllianakis (2010) another research the complication rate in wire insertions were 3.8% in a 20 patient specimen.

Several studies are indicating that many non unions occur during MRSA or osteomyelitis, regarding to insufficient fracture treatment. According to Antonova (2013) this percentile appears to be 12% in the United States regarding Tibia fractures.

2.3 Ilizarov's Design

Ilizarov apparatus is designed in a way to produce a trampoline effect on the fracture ends and this way accelerating the osteogenesis process. This effect is taking place without affecting the rigidity of the assembly. The small diameter of the wires and morphology are ideal for small segments of bone to be captured without the need of an open surgery and therefore minimum damage is caused to the soft tissues. This minimum invasive technique is resulting to immediate blood supply from the vessels to the fracture area.

Several parts with multipurpose designations can be used on the Ilizarov external fixator like hinges shown in Figure 6, conical washers shown in Figure 7, plates, threaded rods and universal joints presented in Figure 8. By the use of these components almost infinite number of variations occurs, depending on the task. With the appropriate configuration bone segments can be moved in any direction correcting problems of length, angulations and rotation.

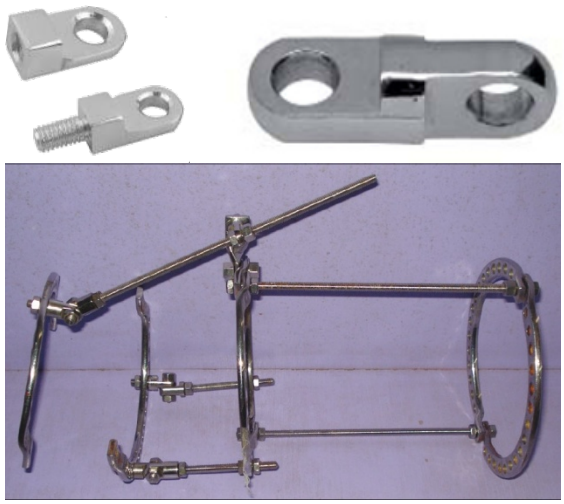

Figure 6 Ilizarov Hinge Assembly

Figure 7 Conical Washer assembly

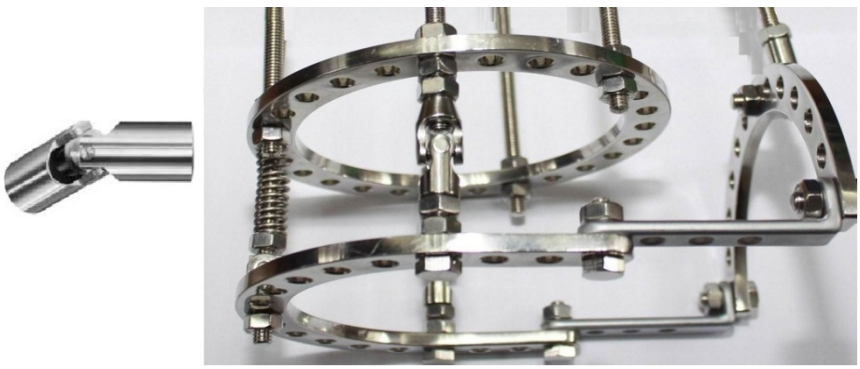

Figure 8 Ilizarov frame with cardanic joints

2.4 Biocompatible Materials

Ilizarov apparatus is an external fixator designed to hold the fracture segments rigidly and in a proper alignment until the healing of the fracture. To do so, thin k-wires are implanted into the bone which are tensioned to achieve the proper stiffness for the healing process to follow. The k-wires are attached to the external rings by special clamps in order to attain tension and therefore their stiffness. This frame-bone interface is resulting complicated mechanical loads. In order to withstand these loads the frame and the k-wires must be manufactured from the proper materials concerning also the performance environment.

The environment that these materials are expected to perform is a hostile one. Human body contains several fluids in different tissues which PH varies from 1 to 9. During daily activities bones are experiencing stresses up to 4 MPa, while tendons who are responsible for certain movements of the bones are subjected to stresses up to 80 MPa. Another important factor to be considered is that these stresses are repetitively and undulated causing fatigue to the materials. It should be mentioned that the described biological environment is mostly depending on the individual patient's daily activities. (S. Ramakrishna, 2001)

Considering the mentioned environment of performance, the material selection process for an external fixator is limited to biocompatible materials with increased stiffness, fatigue strength and ductility. Biocompatible materials (biomaterials) are artificial or natural materials that have been used to supplement or replace functions of human tissues. Their use is known from the ancient times. Their selection was a result of trial and error process which usually led to the rejection of them from the human body. Over the years with the evolution of science and medicine the words biomaterial and biocompatibility have been coined to describe the biological performance of the material. Extended use according to the gained knowledge, of biomaterials, is leading to the patients improved life quality. Responsible for this improvement is the proper design and manufacture of sophisticated implants and medical devices.

Biomaterials according to (S. Ramakrishna, 2001) are categorized as metals and their alloys, ceramics, polymers and composites:

- The category of metals and alloys include stainless steel, Ti alloys, gold, Co-Cr, tantalium and NiTi shape memory alloy. They are characterized by high mechanical strength, ductility and wear resistance. On the other hand they are low biocompatible, while they can release metal ions causing an allergic reaction to the tissues. They also have high density and increased stiffness compared to the tissues, a fact that results their use in hard tissue applications. Finally they are radio opaque causing the appearance of non desirable volumes on the X-ray plates.
- Ceramics like Alumina, zirconia and carbon are also extensively used. They are used mostly in hard tissue applications. They appear to have very good biocompatibility, corrosion and compression resistance. Their drawbacks are brittleness, low fracture toughness, high density and low mechanical reliability.
- Polymers like polyethylene (PE), polyurethane (PU), polyethylene terepthalate (PET) and polyethererketone (PEEK) are used both in hard and soft tissue applications because of their properties. The properties of polymers can vary depending on their composition. They are radio transparent, a very important advantage when it comes to post operative monitoring through x-rays or tomography.
- Composite biocompatible materials such as silica (Si), carbon fiber epoxy (CFRP) and carbon fiber - ultra high molecular weight polyethylene (CF/UHMWPE) are used mostly in orthopedic applications. Composites like polymers are radio transparent; they have increased fatigue resistance, low modulus of elasticity, high strength, and by controlling the arrangement of the reinforcement phase, implant design can be tailored to meet the host tissues specifications. (S.Ramakrishna, 2001)

In common practice, Ilizarov External ring Fixator is manufactured out of stainless steel or titanium alloys. Taking advantage of the stress stiffening effect that occurs during the k-wires pretension the desirable rigidity of the apparatus is achieved. High strength, ductility and wear resistance of these metallic biocompatible materials are crucial for the bone formation and fragment healing. Carbon fiber epoxy is also used for the manufacture of the apparatus in order to

take advantage of its exceptional mechanical properties. The fact that CF/Epoxy is radio transparent results in more accurate x-ray images during the post operative distraction osteogenesis process.

3. Methodology

3.1 Methodology Review

For the present study, a reliable numerical model is going to be developed. This will help the understanding of the process and will contribute in the achievement of the best possible adjustments for each stage of the osteogenesis process. For this, a realistic 3D model which corresponds to the actual geometry is required. The 3D model is going to be designed in Solidworks software. Two assemblies are going to be designed. The diameter of the half rings and the threaded rods will be the same for both files, but the k-wire diameter will differ. The first assembly will include 1.8 mm thin wires, while the second will consist of 2 mm k-wires

The modeled geometry is going to be directly inserted in the FEA software Ansys Workbench via the CAD configuration manager available in Ansys, where the FEM model is going to be produced.

Boundary conditions are going to be set in the model along with the applied loads. The produced models will be loaded with 5 different wire pretension loads according to literature. Two load steps will be used in order to distinguish the pretension load effect on the Femur – frame interface, from the equivalent load that occurs after the dead weight load is applied. The dead load for a femur fragment will be the weight of the knee lower leg and foot.

The materials that are going to be modeled and appear in Table I are 316 stainless steel, Titanium alloy and carbon fiber/PEEK. The material selection is made in order to investigate the differences of the three frames that are available in the market. In Table II are listed the models to be studied.

Table I Material Properties

Materials	Properties			
	Young's Modulus (GPa)	Poison's Ratio	Mass Density (kg/m^3)	Yield Strength (MPa)
316 Stainless Steel	193	0.31	7750	207
Ti-6Al-4V	96	0.36	4620	930
CF/PEEK	75	0.3	1770	4410

Finally, the results of the conducted studies will be evaluated and compared in order to gain knowledge of the different material behavior under the applied load.

3.2 3D modeling

It is necessary to model a realistic representation of the femur – Ilizarov fixator geometry in order to attain the most accurate solution possible. The femur geometry was captured by QCT scans in several planes in a distance of 0.5 mm. The DICOM (Digital Imaging in Communications and Medicine) files were processed by Mimics software, where the segmentation of the digital images took place. After the completion of the segmentation process, the reconstruction of the segment digital images have been done. During segmentation, all the slices are joined in order to produce the 3D geometry. This geometry was exported in a STEP format. After the proper capture of the femur 3D geometry, the model was inserted into Solidworks, where the fragment of the bone was modeled, by separating the bone in three segments. Furthermore the necessary k-wires holes have been modeled to the distal and proximal bone. The final femur model consists of three components. Two of these components are representing the cortical bone and the third one the cancellous bone tissue at the fragment area after the corticotomy.

Different areas of the femur vary in mechanical characteristics and therefore it is necessary to include them in the model as shown in Figure 9.

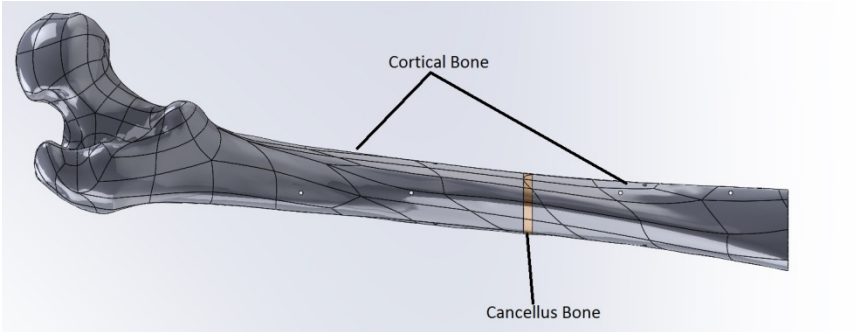

Figure 9 Femur bone

The Ilizarov apparatus was also modeled in Solidworks. The fixator's external rings that have been designed have an external diameter of 180 mm and 6 mm thickness, representing this way a variation of the apparatus, described in the literature. The k-wire clamps were included in the ring geometry since the pretension loss after dynamic loading is not going to be studied. This simplification of the geometry was also critical concerning the computing resources used, during the solution of the model in Ansys. The k-wires were also modeled in Solidworks in two variations, one of 1.8 mm diameter and one of 2 mm. The model of a single external ring consists of four parts. These parts are the two half rings and two k-wires placed in a 90 degrees intersection.

Two variations of the previous model have been produced. The first variation includes two 1.8 mm k-wires and the second one consists of two 2 mm k-wires.

The distal and proximal fragment area fixation rings were modeled paying extra care to the proper alignment with the femur. The rings close to the fragment area were placed in 40 mm distance from the fragment.

Two ring subassemblies connected with threaded rods have been used for each femur segment. Threaded rods are equally distributed around the ring perimeter. The morphology of the femur made the perfect alignment impossible and therefore a small deviation concerning the center plane of the wires can be observed.

The proximal bone ring subassembly is connected to the distal one by four 120 mm long threaded rods. The diameter of all threaded rods used was 6 mm.

The final model shown in Figure 10 consists of:

- Eight half rings.
- Eight 1.8 mm thick k-wires.
- Eight 75 mm long threaded rods.
- Four 120 mm rods.
- Femur model.

The femur model can only move lengthwise to each wire. The 90 degree angle between the wires is eventually restricting the femur movement. The material of the femur-fixator I model is stainless steel 316.

Following the same procedure, the rest of the Ilizarov Frame variations have been modeled. In the following table variations of the ilizarov frame to be studied are listed.

Table II Modeled Ilizarov frames for this study

Fixator Model	Ring Diameter	k-wire pretension loads (N)	K-wire Diameter	Material
Fixator I	180 mm	500,700,900,1100,1300	1.8 mm	316 Stainless Steel
Fixator II	180 mm	500,700,900,1100,1300	2 mm	316 Stainless Steel
Fixator III	180 mm	500,700,900,1100,1300	1.8 mm	Ti-6Al-4V
Fixator IV	180 mm	500,700,900,1100,1300	2 mm	Ti-6Al-4V
Fixator V	180 mm	500,700,900,1100,1300	1.8 mm	CFRP
Fixator VI	180 mm	500,700,900,1100,1300	2 mm	CFRP

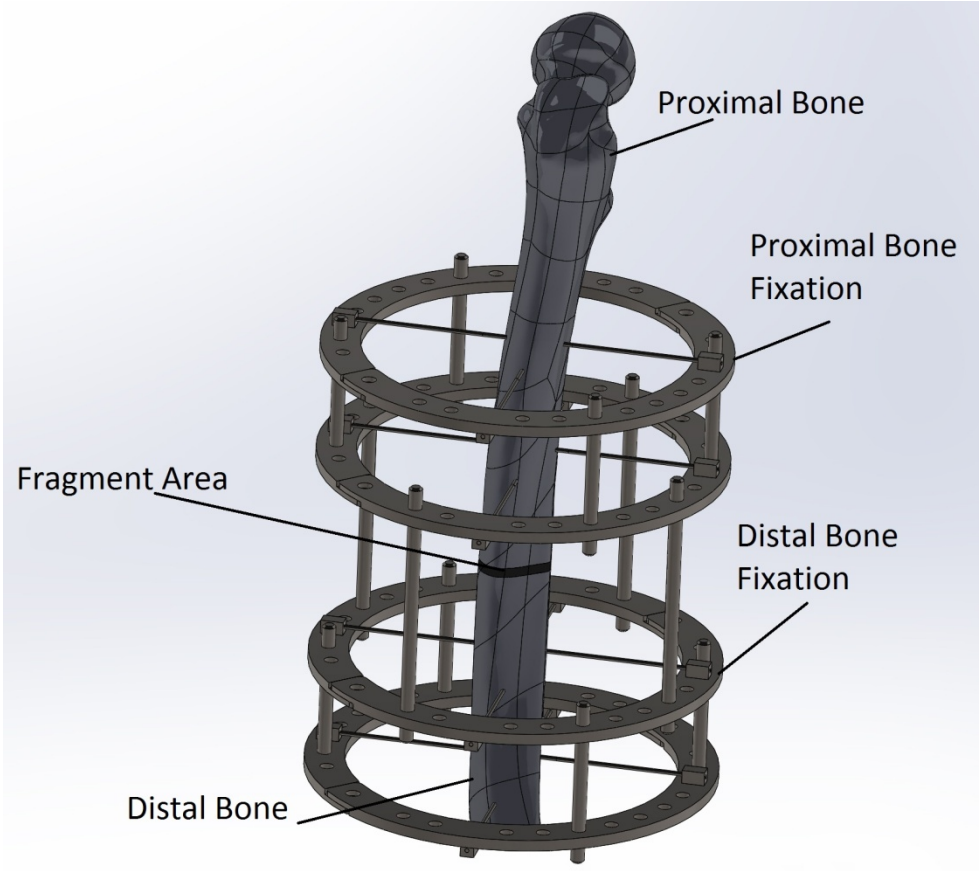

Figure 10 Final 3D model presentation

3.3 FEM Model

Finite element computing software Ansys 14.0 (Ansys Inc. Canonsburg, PA, USA) was used for the computational modeling. The FEM model was modeled and computed in workbench interface of Ansys software package. The k-wires were discretized by 1 mm Hexagonal elements Hex20 following the sweep method. Hex 20 elements were selected in order to achieve optimal solution efficiency and accuracy in the area of the k-wires. Tetrahedral elements Tet10 were used to describe the femur geometry. Tet10 elements were also used on the threaded rods and ring geometry. These surfaces have been mapped by pointing the squarish topologies, wherever they were located, in order to achieve a more uniform mesh with fewer nodes. Local mesh controls took place to the k-wire openings of the femur. By the use of smaller elements and denser mesh, more accurate results can occur on the wire-bone interface. The overall mesh graphic representation is shown in Figure 11 and the established metrics are shown in the diagram of Figure 12.

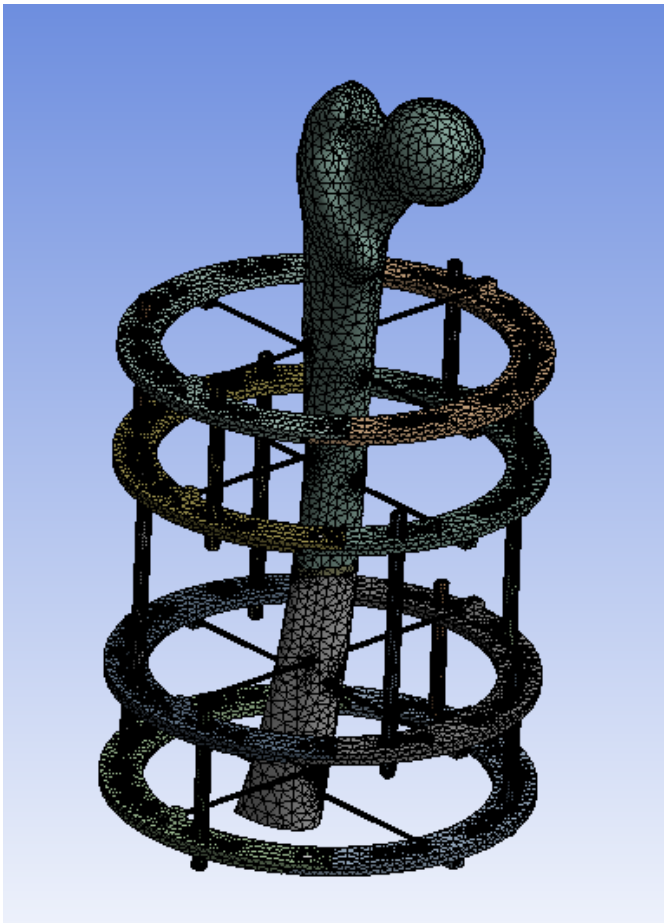

Figure 11 – Mesh Graphical representation

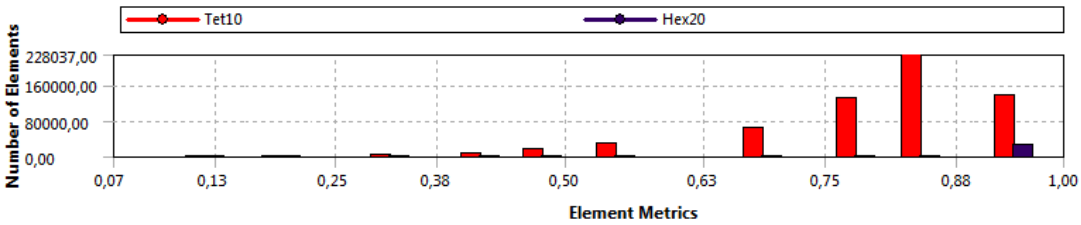

Figure 12 –Mesh element metrics

Contact elements are automatically detected when two separated surfaces are tangent. These contacts must be established in the software in order to achieve contact compatibility. Contact compatibility is the state during which surface interpenetration is prevented. The importance of contact elements is demonstrated by the FEA model of K. Karunratanakul (2010) resulting to errors up to 46% under non accurate contact elements.

Contact elements with zero degrees of freedom have been used where there is no relevant movement between the bodies. Such connections have been set to be the threaded rods-external ring interface and the k-wires-ring interface assuming that no

slippage under dynamic load occurs. Furthermore, the contact between femur bodies have been limited to 0 degrees of freedom in order to stabilize the model and have this way a clear solution result on the fragment area.

Femur-k-wires contacts have been set to "No separation" restricting this way the radial movement of the femur to the wires, preventing any kind of penetration of the two geometries. Axial movement of the femur along each k-wire is allowed along with the rotation around each wire axis.

3.4 Material Modeling

Bones have a complex internal and external structure. Their tissues are characterized by inhomogeneity and anisotropic non linear behavior. These mechanical characteristics are very difficult to be modeled. The material model used for this study, is homogeneous, linear and isotropic according to similar studies. This kind of material is described by the modulus of elasticity and Poison's ratio.

Femur like other bones consists of cortical and cancellous tissue. For the conduction of this study it has been assumed that femur is hollow with no cancellous tissue in its overall length. Such an assumption is made because cancellous bone tissue is highly heterogenous and according to Prendergast (1997) research it has to be considered as homogenous continuum. Such an assumption would slightly differentiate the results but because of cancellous bone low modulus of elasticity it was chosen to be excluded from the conducted study. Cancellous bone tissue was added only to the fragment area in order to get a graphical representation of it, and stabilize our model, allowing for an easier convergence..

Many different values of young's modulus and poison ratio can be found in literature. Young's modulus varies from 15 to 20 GPa and Poison's ratio v=0.4 for cortical bone tissue, while for cancellous bone Young's modulus varies between 0.2-13.9 GPa and poison's ratio to 0.3.

For the conducted study, the following properties have been used according to Georgadakis study (2010):

- Cortical bone Young's modulus: 18.6 GPa and Poison's ratio: 0.4
- Cancellus bone Young's modulus: 0.2 GPa and Poison's ratio: 0.3

3.5 Model of load and boundary conditions

The fragment width in our model is about 4 mm. In such situations patients are not allowed to load the affected limp. Therefore crunches must be used for walking. The use of crunches results to the load of the femur- fixator interface only by the dead weight. In the case of femur fragment, the dead load is the weight of the knee, lower leg and foot. This dead weight has been considered to be 200 N. The state of load to be studied is the one that the patient hangs his leg while walking with crunches. The model has been restricted by eliminating all degrees of freedom to the hip joint area.

3.6 Model Convergence

There are numerous quality mesh metrics that can be computed. These metrics are very important since mesh quality affects convergence more than accuracy. The metrics that have been used for the studied model was the orthogonal quality of mesh elements. The 892326 nodes constitute 563594 elements. The minimum orthogonal quality was 0.075 and the maximum was 0.995, resulting to an average value of 0.808. The exact element metrics are shown in Figure 12.

After the orthogonal quality metric check the model mesh have been converged. By the term converged mesh it is defined the mesh quality by which increment, negligible result variation occurs. Model has been solved with different mesh qualities and element sizes, starting from a coarser mesh. The results of each study were compared to each other in order to calculate the deviation percentage. This result deviation percentage set to be 1% for a mesh quality to be acceptable. After several solutions with finer mesh each time, it was observed that the results deviation convergences to 1%. The coarser mesh of the solutions, which result deviation was less than 1%, was then selected as optimal, for the studied model.

4. Results

4.1 Deformation of the System

The FEM model has been set up according to paragraph 3 of the present study; the boundary conditions are shown in Figure 13. The bone is being restricted at the hip joint area, force B is applied to the lower cut surface of the femur along Y axis, which lies throughout the frame height. The pretension loads are applied along k-wires in X and Z axis. The model is initially subjected to the k-wire pretension. The fixed k-wires are loaded in 5 different pretension loads. Figure 14 shows the total deformation of the system studied. According to the color scale, the largest deformation appears in red color while the minimum is shown in blue. The following graphical representations are corresponding to 2 mm stainless steel k-wires tensioned at 500 N, and they are plotted in a larger scale concerning the appearance of the deformation. This larger scale will help in the better understanding of the problem.

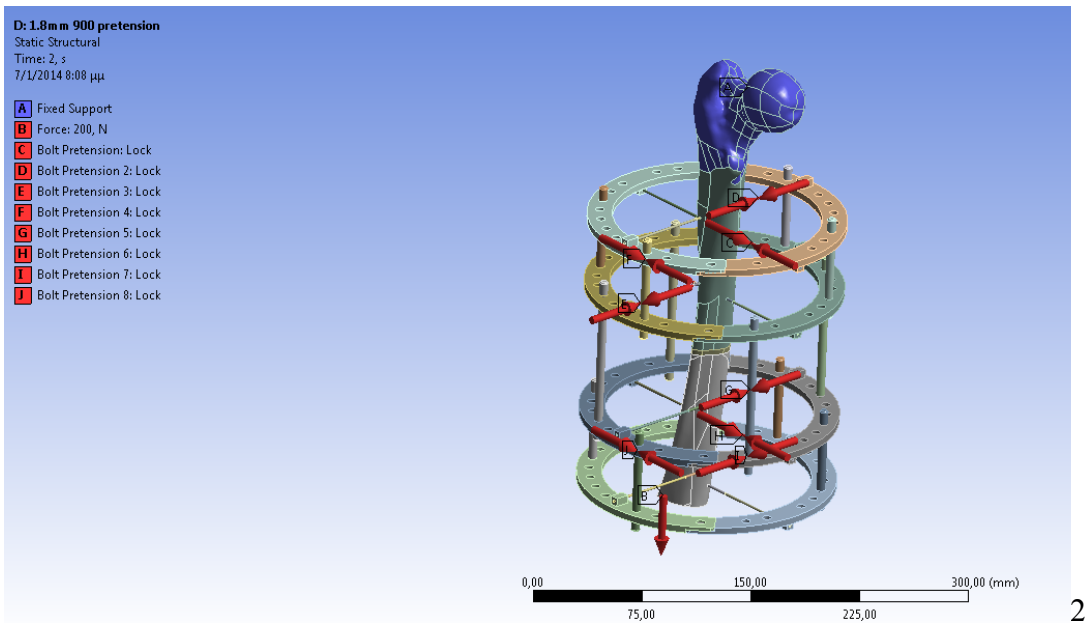

2

Figure 13 Boundary and load representation

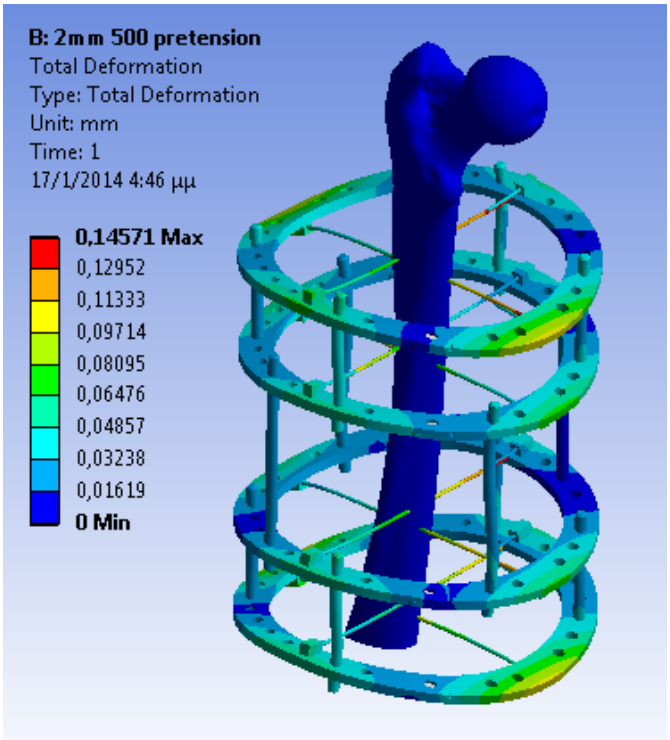

Figure 14 Total Deformation under k-wire pretension load

It can be observed that the applied load is causing the bending of the rings. The axial displacement of the first load step in Y axis which crosses through the height of the apparatus as indicated in Figure 15. The color scale on the axial displacement differs from the total deformation shown in Figure 14. Red color represents the maximum displacement in the positive scale of Y axis while the blue the minimum displacement on the negative scale of the Y axis. It is obvious that the areas of the k-wires attachment are the areas of the largest axial deformation in the system.

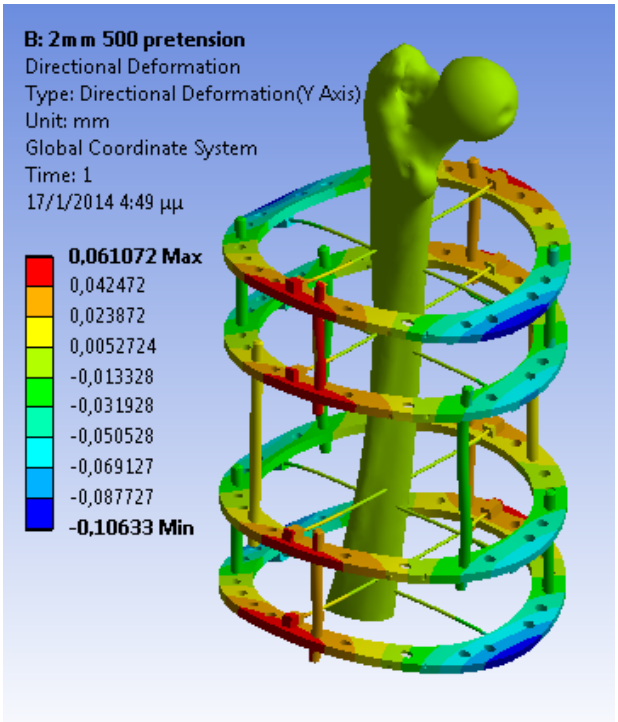

Figure 15 Directional Y Deformation

From the direction of the deformation it can be concluded that it is caused by the k-wire pretension. The deformation of the rings on the Y axis results from the relevant displacement of the two k-wires on the same ring. This profound change in the deformation of the rings on the Y axis, combined with the high stiffness of the k-wires results to local concentration of stresses to the bone area at the k-wires insertion points as shown in Figure 16 and Figure 17. The range of equivalent stress in the system is shown clearly in Figure 16. The location of the maximum values is indicated by the red color and the minimum value is indicated by blue color. The maximum value of equivalent (von Mises) stress of the system shown in Figure 16a is located at the k-wires, and is shown in the detail in figure 16b. By isolating the bone and by plotting the equivalent stress as evidently shown in Figure 17, the maximum value is located on the k-wire insertion points of the proximal bone. Therefore, this is a location that is of prime importance and it is going to be monitored and presented also in graph. This graph will help in the better understanding of the material, pretension and diameter impact on the cortical bone tissue. The interaction between the k-wires and the bone is also going to be studied along with the impact of the various factors under study (k-wire diameter, pretension and material) to the fragmented area.

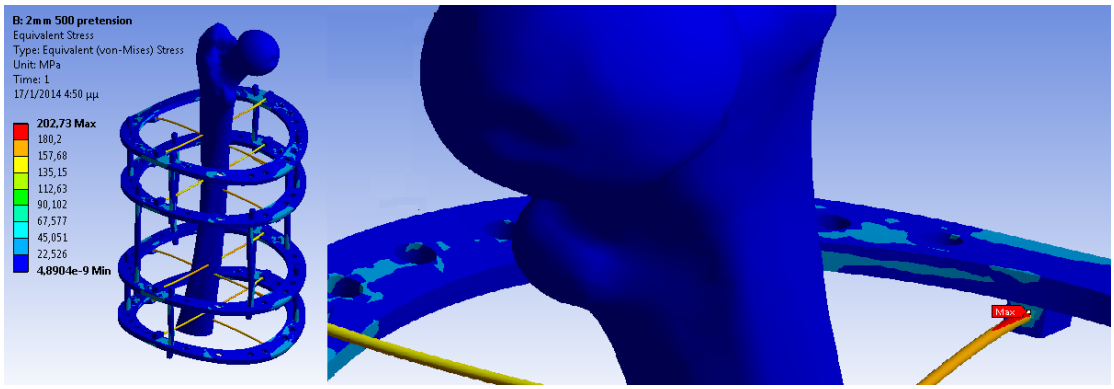

Figure 16 a) Von Mises Stress on the frame. b) Detail of Local Stress Maximum

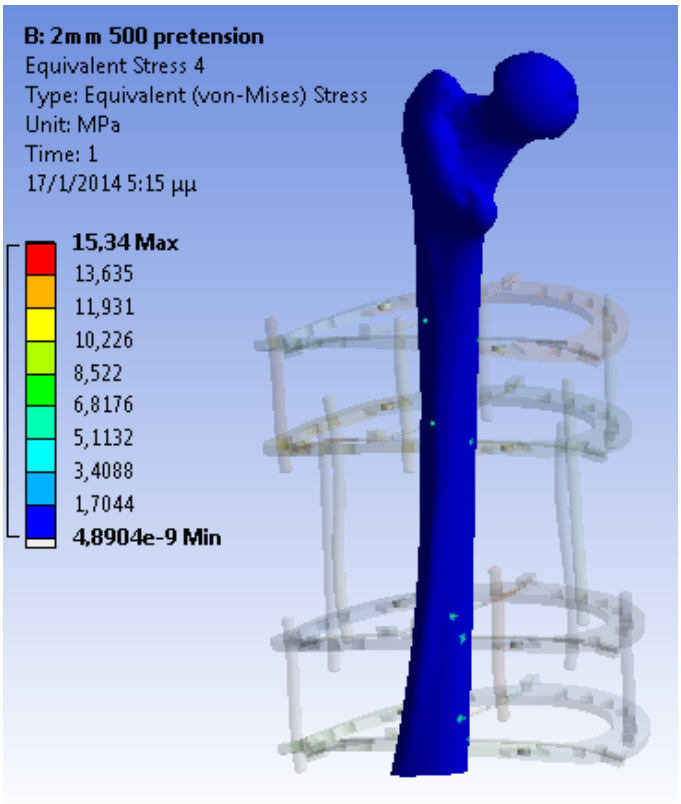

Figure 17 Von Mises Stress on the Femur caused by k-wire pretension.

During the second load step the k-wire pretension is sustained and the dead weight is added to the model. Because of the femur geometry, it was impossible to be completely aligned with the frame. Femur is stabilized at the hip joint area which is not lying on the same axis as the tibia and calf. Therefore, after the dead load was applied to the model, the frame tended to bend. This is obvious on Figure 18 where the total deformation of the system is presented.

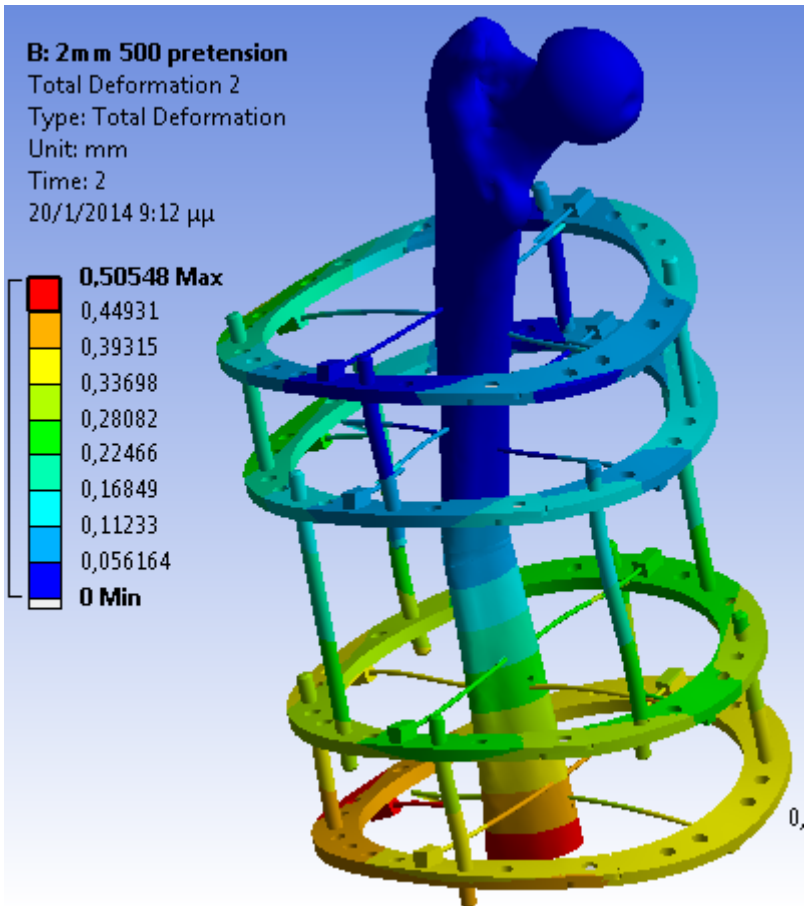

Figure 18 Total Deformation under Equivalent Load

This deformation caused by the dead weight bearing, occurs to all axis and it is monitored by the deformations that take place to the fragmented area of the cancellous bone as shown in Figure 19.

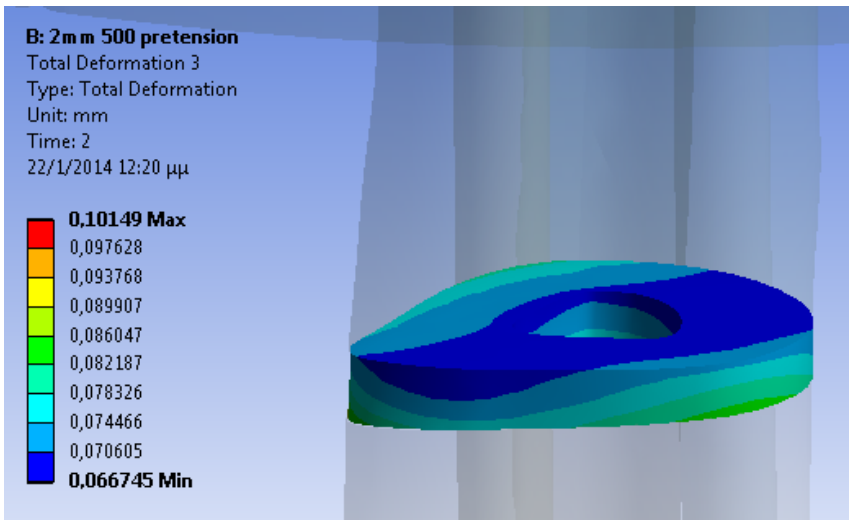

Figure 19 Fragment Area Total Deformation

The directional deformation in the Y axis shown in Figure 20, during the second load step is not symmetrical due to the fact that the dead weight load lies on a different axis than the support of the hip joint area.

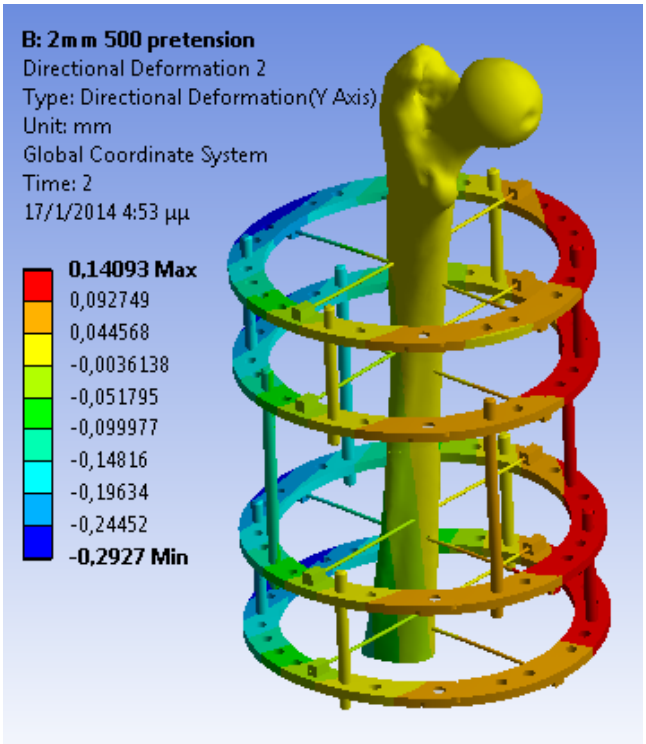

Figure 20 Axial Y Deformation

The equivalent stress of the frame-femur system shown in Figure 21 is also changing if it is compared with the first load step, but because of the small value of the dead weight this difference is relatively small.

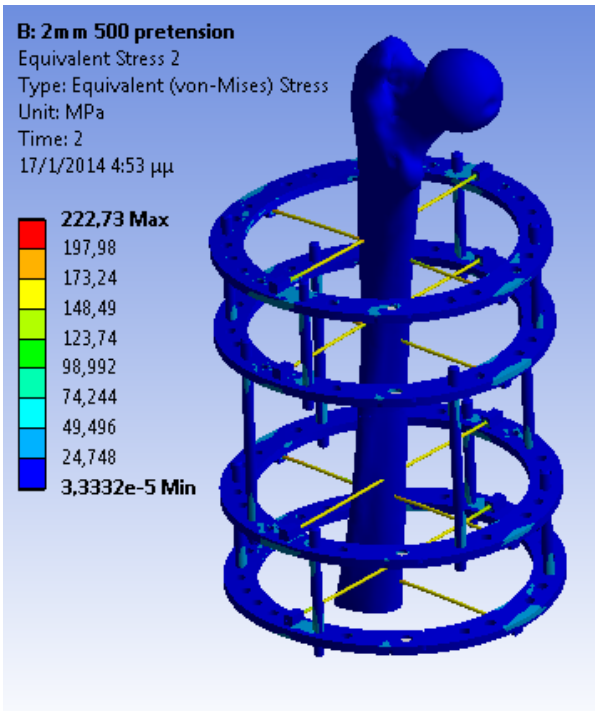

Figure 21 Von Mises Stress on the Frame in Load State 2

The impact of the dead bearing load from the bone at the insertion points of the k-wires as shown in Figure 22, is very small and as it will be observed in the following

paragraphs and to the aggregated results of this research, it appears to be favorable for the bone.

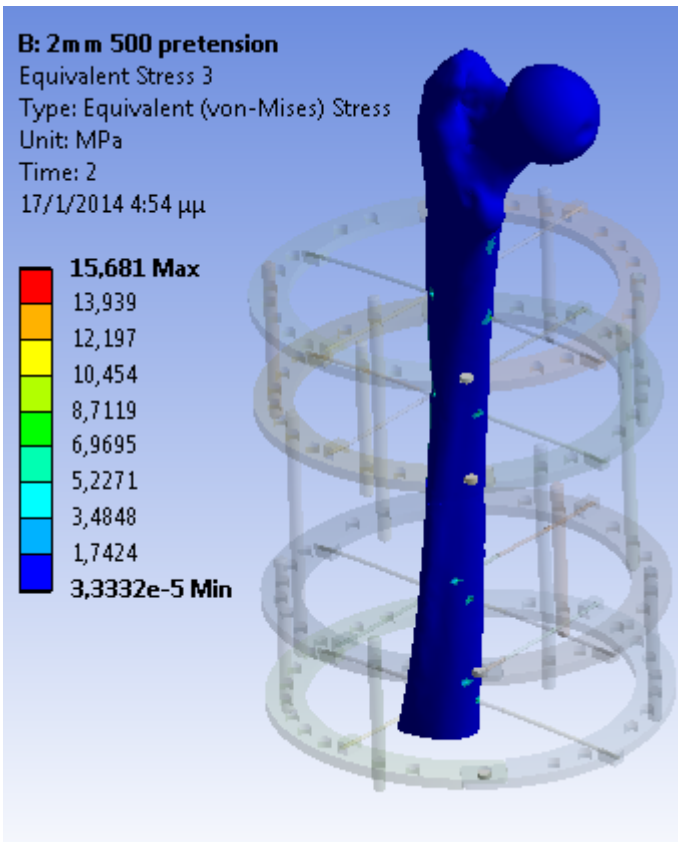

Figure 22 Von Mises Stress on the Femur caused Equivalent Load.

4.2 Comparative Results

After the surgical procedure described in paragraph 2.2 the k-wires are tensioned to the desired load. In this chapter the results of the conducted studies shown in Table II will be presented.

Because of the k-wires tension, the frame is initially deformed. The values of the overall deformation (in mm) of the system are shown in Table III.

Table III Total deformation (in mm) of the frame under k-wire pretension load

	BOLT PRETENSION (N)				
FRAME	**500**	**700**	**900**	**1100**	**1300**
1,8mm SS	0,16673	0,23385	0,30048	0,36718	0,43317
1,8mm Ti	0,33688	0,47394	0,60915	0,74477	0,87918
1,8mm CF/PEEK	0,43305	0,60553	0,77828	0,95328	1,1267
2mm SS	0,14571	0,20382	0,25991	0,31632	0,37301
2mm Ti	0,2907	0,4029	0,5177	0,63272	0,7472
2mm CF/PEEK	0,36797	0,51415	0,66159	0,80896	0,95557

In Table III left column, the type of the frame is appearing while on the horizontal, the k-wire tension load (Bolt Pretension in Newton (N)). It can be concluded that the smallest deformation is appearing on the stainless steel frame, while the largest one on the CF/PEEK frame. This difference in deformation occurs due to the higher modulus of elasticity of stainless steel, as shown in Table I. Total deformation of the system shown in Table III is taking place in all axis and therefore the results of the directional deformation in Y axis will be needed, in order to investigate the relative displacement of the k-wires to the rings. This relative displacement seems to create stress concentrations on the femur, on the k-wire insertion points, as have been indicated in section 4.1. The directional displacement in Y axis is appearing on Table IV.

Table IV Directional deformation of the frame under k-wire pretension load on Y axis

	BOLT PRETENSION (N)									
FRAME	**500**	**500**	**700**	**700**	**900**	**900**	**1100**	**1100**	**1300**	**1300**
	MIN	**MAX**	**MIN**	**MAX**	**MIN**	**MAX**	**MIN**	**MAX**	**MIN**	**MAX**
1,8mm SS	-0,1062	0,0593	-0,1453	0,0842	-0,1861	0,1107	-0,2269	0,1376	-0,2676	0,1644
1,8mm Ti	-0,2155	0,1261	-0,2953	0,1787	-0,3803	0,2342	-0,4660	0,2909	-0,5518	0,3476
1,8mm CF/PEEK	-0,2743	0,1653	-0,3747	0,2309	-0,4837	0,3023	-0,5960	0,3789	-0,7084	0,4534
2mm SS	-0,1063	0,0611	-0,1474	0,0876	-0,1886	0,1139	-0,2297	0,1406	-0,2710	0,1676
2mm Ti	-0,2134	0,1285	-0,2977	0,1826	-0,3831	0,2383	-0,4691	0,2945	-0,5558	0,3509
2mm CF/PEEK	-0,2698	0,1656	-0,3775	0,2368	-0,4872	0,3078	-0,5983	0,3808	-0,7108	0,4567

The total deformation of the frame shown in Table III can be presented in a graph in order to have a clear picture of the effect of k-wire tension load, on the deformation of the different frames. In Figure 23 it is evident that the k-wire pretension load increases in a linear fashion with the frame deformation .

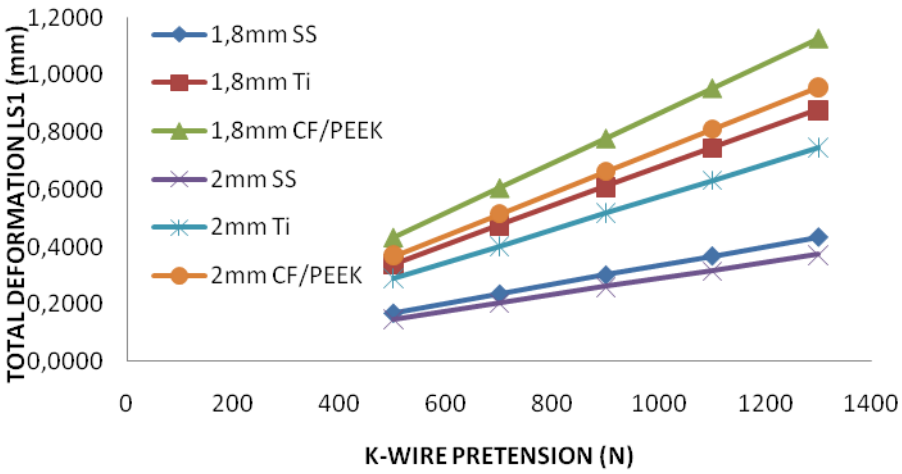

Figure 23 Total deformation of the frame under k-wire pretension load

The maximum equivalent (von Mises) stress values have been inserted in Table V. As mentioned in section 4.1, these maximum values are located to the k-wires, shown in Figure 16a and Figure 16b. The units are in MPa.

Table V Equivalent (von Mises) stress on the frame under k-wire pretension load

	BOLT PRETENSION (N)				
FRAME	**500**	**700**	**900**	**1100**	**1300**
1,8mm SS	249,8	353,41	461,05	570,88	681,95
1,8mm Ti	262,94	367,43	482,25	601,05	720,85
1,8mm CF/PEEK	271,53	377,8	496,4	619,5	743,25
2mm SS	202,73	289,1	377,41	468,49	560,72
2mm Ti	209,81	301,67	397,12	495,85	598,41
2mm CF/PEEK	215,3	310,84	409,32	511,8	619,15

Table V corresponds to the results shown in Figure 24, presenting the von Mises stress growth depending on the k-wire diameter and material. Comparing the maximum values of the von Mises stress with the yield strength values of Table I, it can be concluded that for stainless steel k-wires, the maximum equivalent stress exceeds the yield strength under all tension loads. Clearly, a permanent deformation of the stainless steel k-wires occurs. This result agrees well with the findings from the work of P.J. Hillard (1998) and La Russa (2011). The maximum values are corresponding to the maximum equivalent stress located on the k-wires, as shown in Figure 16a and Figure 16b.

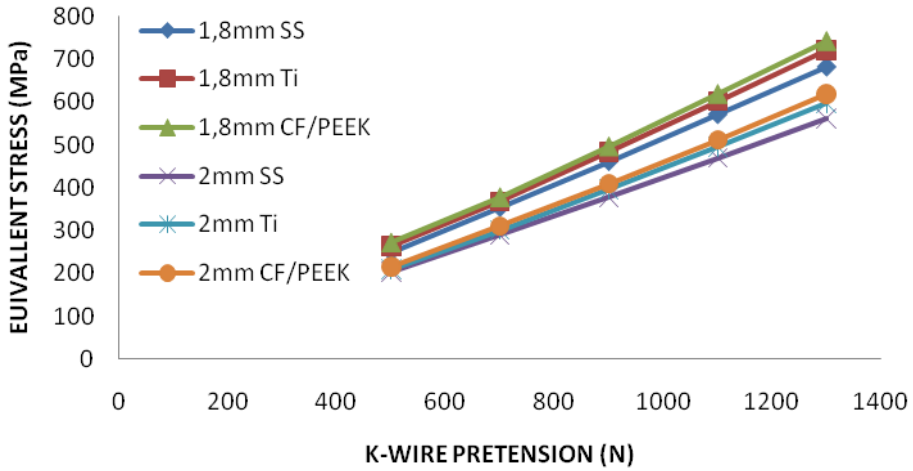

Figure 24 Equivalent (von Mises) stress on the frame under k-wire pretension load

The results of the total deformation of the rings (isolated) are shown in Table VI, during the first load step (k-wires tension load). This total deformation along with the directional deformation of the ring on Y axis, presented in Table VII, will help in the understanding of the impact of the k-wire displacement on the femur during the first load step.

Table VI Total deformation of the rings during 1st load step

	BOLT PRETENSION (N)				
FRAME	**500**	**700**	**900**	**1100**	**1300**
1,8mm SS	0,1064	0,1483	0,1897	0,2312	0,2724
1,8mm Ti	0,2149	0,3000	0,3861	0,4730	0,5601
1,8mm CF/PEEK	0,2725	0,3810	0,4916	0,6044	0,7183
2mm SS	0,1071	0,1485	0,1901	0,2318	0,2735
2mm Ti	0,2149	0,3001	0,3864	0,4734	0,5614
2mm CF/PEEK	0,2719	0,3806	0,4918	0,6044	0,7180

Having in mind the modulus of elasticity of the studied materials as illustrated in Table I, it is obvious that the rings having materials with the higher Young's modulus are deforming less for the same tension of the k-wires. This conclusion is better shown in Figure 25.

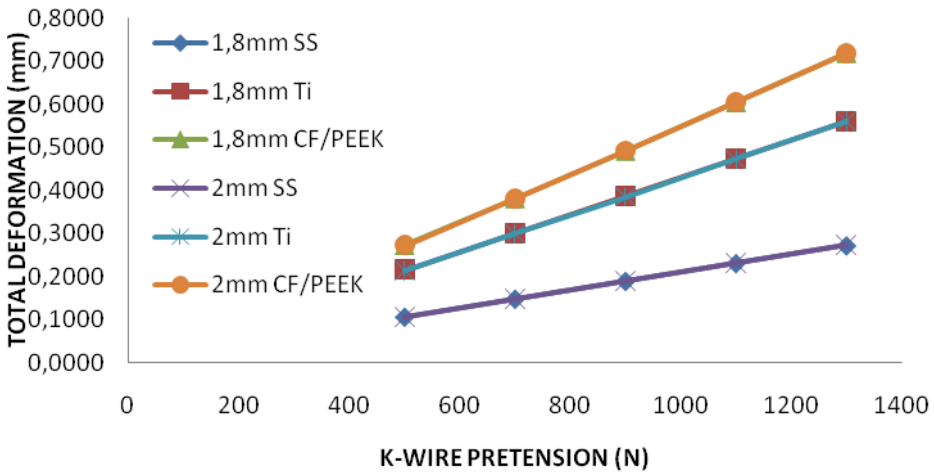

Figure 25 Total deformation of the rings during first load step

It can be observed in Figure 25 that the total deformation of the rings is the same, irrespective of the material used and this deformation is irrelevant to the k-wire diameter.

The ring directional deformation on Y axis is shown in Table VII. This deformation is very important, since it causes stress concentrations at the k-wires insertion points (on the femur). This directional deformation that is not symmetrical concerning the k-wire clamping areas, can also be observed in Figure 20. This happens owing to the threaded rods location, connecting the proximal bone rings. The maximum and minimum values of directional deformation are located at the k-wire attachment points to the rings.

Table VII Directional deformation on Y axis of the rings

	BOLT PRETENSION (N)									
FRAME	500	500	700	700	900	900	1100	1100	1300	1300
	MIN	MAX	MIN	MAX	MIN	MAX	MIN	MAX	MIN	MAX
1,8mm SS	-0,1057	0,0593	-0,1453	0,0842	-0,1861	0,1107	-0,2269	0,1376	-0,2676	0,1644
1,8mm Ti	-0,2135	0,1261	-0,2953	0,1787	-0,3803	0,2342	-0,4660	0,2909	-0,5518	0,3476
1,8mm CF/PEEK	-0,2709	0,1648	-0,3747	0,2309	-0,1298	0,1495	-0,1628	0,1804	-0,1933	0,2138
2mm SS	-0,1063	0,0611	-0,1474	0,0876	-0,1886	0,1139	-0,2297	0,1406	-0,2710	0,1676
2mm Ti	-0,2134	0,1285	-0,2977	0,1826	-0,3831	0,2383	-0,4691	0,2945	-0,5558	0,3509
2mm CF/PEEK	-0,2698	0,1656	-0,3775	0,2368	-0,4872	0,3078	-0,1767	0,1659	-0,2093	0,1974

In order to investigate if the rings are deforming permanently under the pretension load, the minimum values of the safety factor will be needed. This safety factor is the result of yield strength divided by the equivalent stress calculated by Ansys.

Table VIII Minimum safety factor of the rings under pretension load

	BOLT PRETENSION (N)				
FRAME	500	700	900	1100	1300
1,8 mm SS	1,9036	1,3891	1,0828	0,8616	0,69747
1,8 mm Ti	8,2442	5,7128	4,2471	3,0746	2,4283
1,8 mm CF/PEEK	15	15	15	13,43	10,514
2 mm SS	2,5193	1,7762	1,3657	1,1042	0,92299
2 mm Ti	11,053	7,6283	5,5378	4,3874	3,5275
2 mm CF/PEEK	15	15	15	15	15

From the results inserted in Table VIII, can be concluded that the stainless steel rings tend to deform permanently under tension at 1100 N and 1300 N of 1.8 mm k-wires, while this happens in 1300 N pretension of the 2 mm k-wire. Figure 26 shows the safety factor for the different conducted studies and its reduction trend as the pretension load increases.

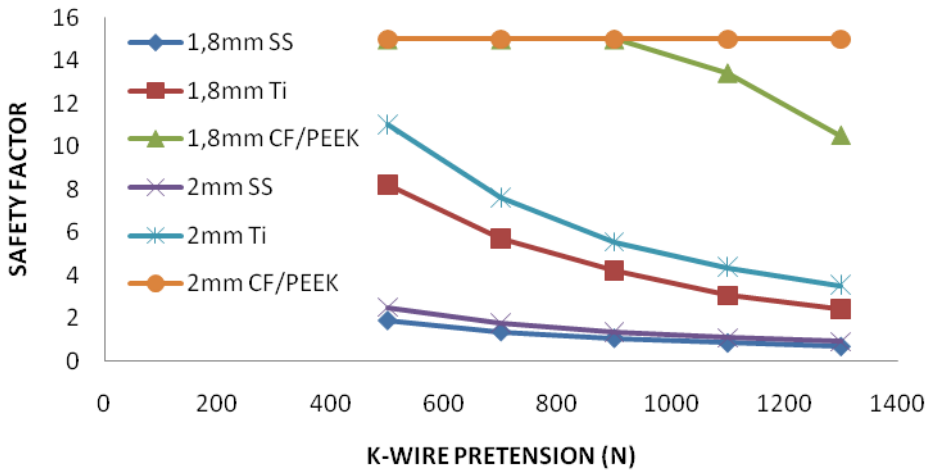

Figure 26 Safety factor of the rings during first load state

The minimum safety factor values for the k-wires shown in Table IX indicate the permanent deformation of the stainless steel k-wires. These deformations occur under tension stress shown in Figure 24, which are higher for the smaller diameter k-wires.

Table IX Minimum safety factor on k-wires during first load step

	BOLT PRETENSION (N)				
FRAME	**500**	**700**	**900**	**1100**	**1300**
1,8 mm SS	0,82866	0,58572	0,44898	0,3626	0,30354
1,8 mm Ti	3,537	2,5311	1,9285	1,5473	1,2901
1,8 mm CF/PEEK	3,705	2,663	2,0719	1,6749	1,4185
2 mm SS	1,0211	0,71602	0,54847	0,44184	0,36917
2 mm Ti	4,4327	3,0828	2,3419	1,8756	1,5541
2 mm CF/PEEK	5,5518	3,9587	3,0697	2,5149	2,1324

The decrement rate of the k-wire safety factor is shown in Figure 27.

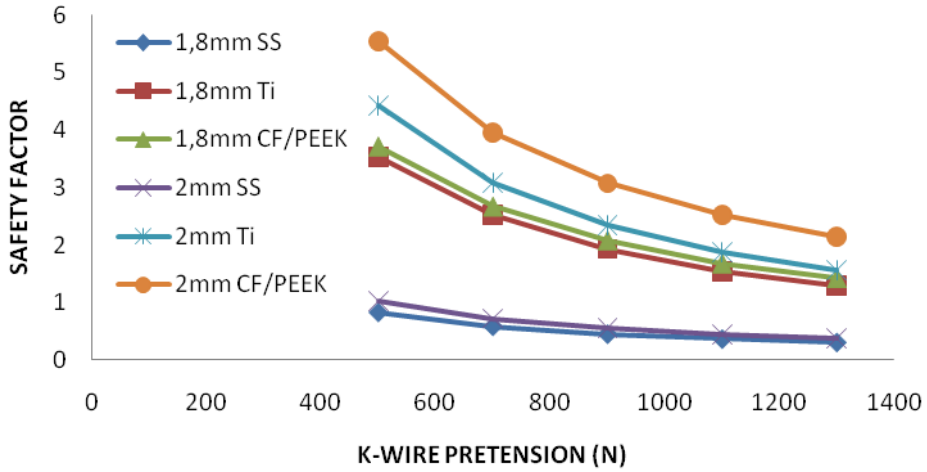

Figure 27 Minimum safety factor on k-wires during first load step

The concentration of stresses on the bone is obvious in Figure 17 and therefore it is useful to observe their values range at this first load step shown in table X.

Table X Maximum equivallent stress on the femur

	BOLT PRETENSION (N)				
FRAME	**500**	**700**	**900**	**1100**	**1300**
1,8 mm SS	22,829	31,652	40,813	50,035	59,237
1,8 mm Ti	53,034	73,98	95,28	116,71	137,86
1,8 mm CF/PEEK	55,871	77,732	99,909	123,59	145,93
2 mm SS	15,34	21,486	27,628	33,773	39,924
2 mm Ti	35,388	49,59	64	78,178	92,168
2 mm CF/PEEK	37,285	52,289	67,434	82,311	97,075

By looking at the maximum equivalent stress results on the femur, it can be concluded that the maximum equivalent stress on femur is depending on the material of the frame and the k-wire tension load. The lower values can be found in the stainless steel rings. Combining these results with the axial deformation of the rings under k-wire

tension shown in Table VII it can be seen that frames with increased axial deformation and small k- wire diameter are causing higher stresses to the femur.

The maximum permissible stress on bones, as described in K.D. Bouzakis (2004) study on a spinal cord bone, appears to be 60 MPa while S. Ramakrishna (2001) sets it to be 133 MPa for the cortical bone. Comparing the results of the current study with the literature it can be seen that stainless steel rings are producing decreased stress values to the femur, while Ti-6Al-4V and CF/PEEK frames especially combined with 1.8 mm k-wires are producing stresses close to the permissible values, as described by W. Walke (2008) 160 MPa on tibia, at high k-wire tension loads. The values of Table X are presented in Figure 28 where stress incensement rate is better shown.

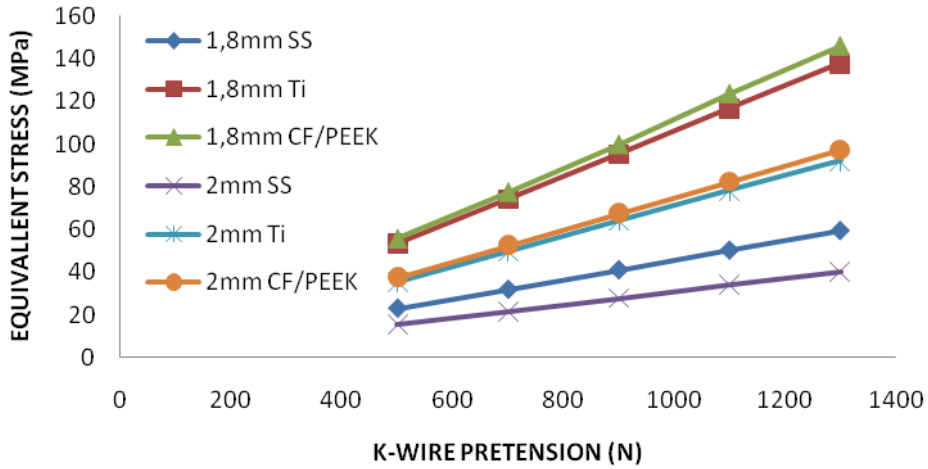

Figure 28 Equivalent Stress on the bone during first load step

The deformation of the rings and generally of the frame, is also affecting the fragment area. The impact of the k-wire tension on the fragment area, is shown on Table XI where the total deformation and consequently the maximum displacement at the fragment area appears.

Table XI Fragment area maximum deformation during first load step

	BOLT PRETENSION (N)				
FRAME	**500**	**700**	**900**	**1100**	**1300**
1,8 mm SS	0,0004	0,0010	0,0013	0,0016	0,0020
1,8 mm Ti	0,0010	0,0019	0,0025	0,0033	0,0041
1,8 mm CF/PEEK	0,0010	0,0021	0,0029	0,0038	0,0049
2 mm SS	0,0006	0,0010	0,0013	0,0017	0,0021
2 mm Ti	0,0013	0,0019	0,0026	0,0033	0,0041
2 mm CF/PEEK	0,0014	0,0021	0,0029	0,0038	0,0049

The deformation values for the fragment area appear to be negligible. It is interesting to see that the difference of these values for the different type of frames end up to be increased by 100% to 150%. This variation can better be observed in Figure29.

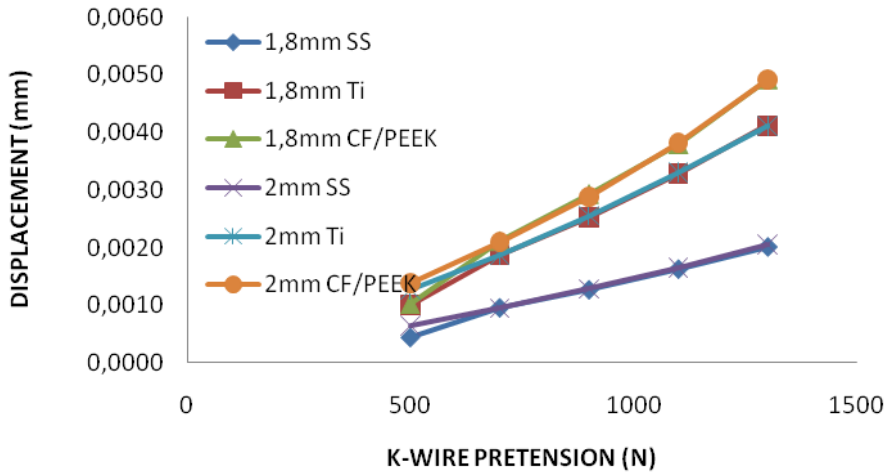

Figure 29 Displacement of the fragment area during first load step

Second load step starts with the application of the dead weight. The total deformation of the frame is shown in Table XII.

Table XII Total deformation of the frame during second load step

	BOLT PRETENSION (N)				
FRAME	**500**	**700**	**900**	**1100**	**1300**
1,8 mm SS	0,5315	0,5316	0,5594	0,6075	0,6629
1,8 mm Ti	0,5307	0,7028	0,8211	0,9409	1,0626
1,8 mm CF/PEEK	0,5307	0,8203	0,9734	1,1288	1,2885
2 mm SS	0,5055	0,5318	0,5594	0,5884	0,6144
2 mm Ti	0,5914	0,6530	0,7294	0,8278	0,9290
2 mm CF/PEEK	0,6362	0,7301	0,8560	0,9840	1,1170

It can be observed that when the k-wires are tensioned to 500 N there is small difference in the displacement of the system between the different configurations of the frame. As the tension increases the total deformation increases also. This happens probably because of insufficient stiffness of the k-wires.

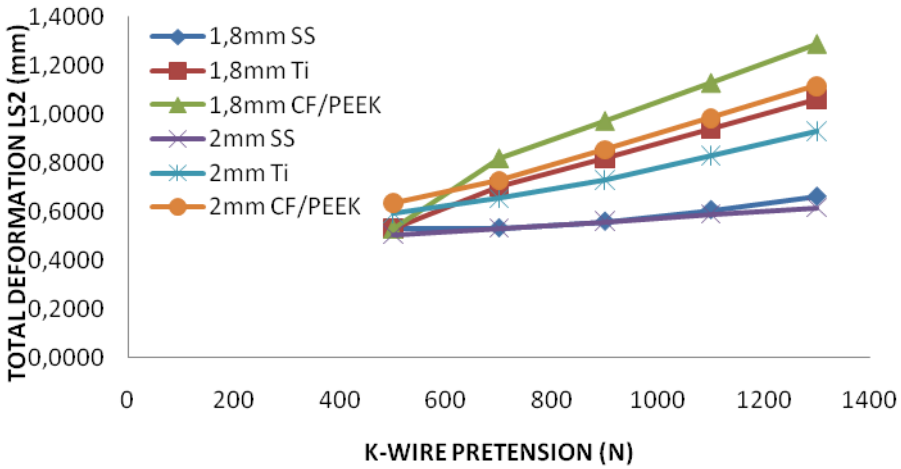

Figure 30 Total deformation of the frame during second load step

The directional on Y axis deformation also increases as a result of the dead weight, and causes bending to the system, as mentioned in section 4.1. In Table XIII the values of this axial deformation are illustrated. The minimum value concerns the negative values in Y axis, while the maximum values the displacement on the positive values of the same axis.

Table XIII Directional on Y axis deformation of the frame during second load step

	BOLT PRETENSION (N)									
FRAME	500	500	700	700	900	900	1100	1100	1300	1300
	MIN	MAX	MIN	MAX	MIN	MAX	MIN	MAX	MIN	MAX
1,8mm SS	-0,1568	0,0593	-0,3245	0,1541	-0,3595	0,1706	-0,3954	0,1897	-0,4286	0,2085
1,8mm Ti	-0,2647	0,1174	-0,4595	0,2259	-0,5353	0,2745	-0,6129	0,3264	-0,6907	0,3791
1,8mm CF/PEEK	-0,3227	0,1546	-0,5308	0,2726	-0,6289	0,3390	-0,7297	0,4081	-0,8336	0,4789
2mm SS	-0,2927	0,1409	-0,3270	0,1507	-0,3618	0,1665	-0,3972	0,1854	-0,4310	0,2036
2mm Ti	-0,3891	0,1789	-0,4632	0,2214	-0,5389	0,2689	-0,6165	0,3204	-0,6951	0,3727
2mm CF/PEEK	-0,4393	0,2078	-0,5350	0,2670	-0,6329	0,3329	-0,7336	0,4018	-0,8384	0,4715

Equivalent von misses stress on the frame shown in table XIV is also increasing as expected on the frame. These maximum stress values are located on the k-wires. It can be observed that these maximum values variation, between the studied configurations of the frame are decreased and significant differences appear between groups of 1.8 and 2 mm k-wire diameter.

Table XIV Maximum von Mises stress on the frame during second load step

	BOLT PRETENSION (N)				
FRAME	500	700	900	1100	1300
1,8 mm SS	249,79	369,45	472,17	577,82	687,59
1,8 mm Ti	262,92	369,62	484,24	601,64	720,98
1,8 mm CF/PEEK	271,51	378,28	497,14	619,06	741,94
2 mm SS	222,73	305,75	390,62	475,31	564,7
2 mm Ti	216,02	303,46	396,25	492,07	590,73
2 mm CF/PEEK	217,83	309,62	406,41	505,75	612,41

This change in the behavior of the k-wires is shown clearly on Figure 31.

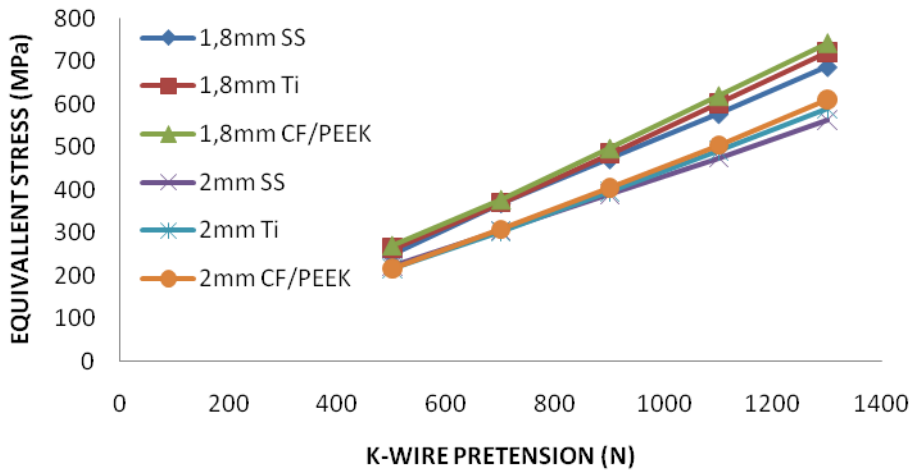

Figure 31 Maximum equivalent stress during second load step

Total deformation of the rings is shown in Table XV, which also increases as the k-wire tension increases. In low tension values though, (i.e. at 500N) pretension for a 1.8 mm k-wire configurations seem to deform less.

Table XV Total deformation of the rings during second load step

	BOLT PRETENSION (N)				
FRAME	**500**	**700**	**900**	**1100**	**1300**
1,8 mm SS	0,1574	0,3265	0,3614	0,3972	0,4304
1,8 mm Ti	0,2646	0,4616	0,5380	0,6162	0,6948
1,8 mm CF/PEEK	0,3214	0,5335	0,6323	0,7341	0,8390
2 mm SS	0,2936	0,3281	0,3632	0,3989	0,4329
2 mm Ti	0,3906	0,4654	0,5417	0,6200	0,6994
2 mm CF/PEEK	0,4413	0,5379	0,6366	0,7383	0,8442

The total deformation of the rings follows the same tendency as in the first load step with the exception of 500 N tensioned 1.8 mm k-wires which deform less than the 2 mm k-wire configurations with the same material. This happens probably because of the low rigidity of the apparatus at this pretension load.

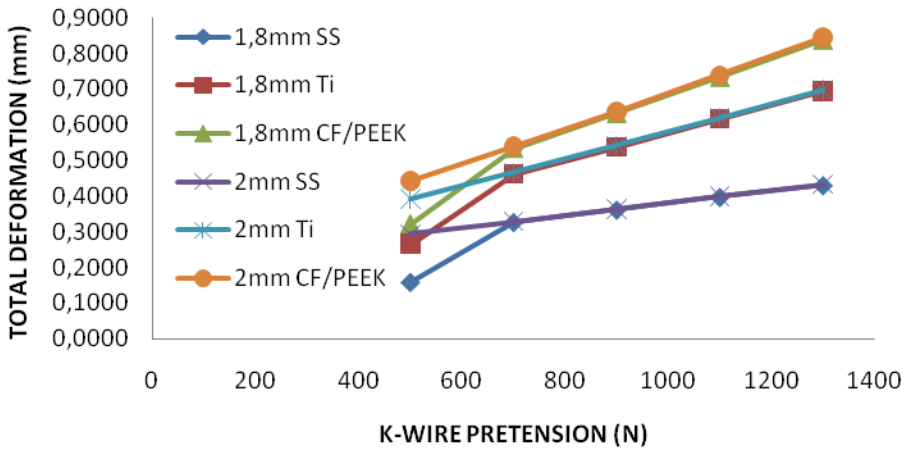

Figure 32 Total deformation of the rings during second load step

The indicated difference in Figure 32 for the 1.8 mm configurations is appearing also in the directional deformation of the rings with the same pattern. The values of the Y axial deformation of the rings are shown in Table XVI.

Table XVI Ring directional deformation during second load step

	BOLT PRETENSION (N)									
FRAME	**500**	**500**	**700**	**700**	**900**	**900**	**1100**	**1100**	**1300**	**1300**
	MIN	**MAX**	**MIN**	**MAX**	**MIN**	**MAX**	**MIN**	**MAX**	**MIN**	**MAX**
1,8mm SS	-0,1563	0,0544	-0,3245	0,1497	-0,3595	0,1666	-0,3954	0,1866	-0,4286	0,2064
1,8mm Ti	-0,2628	0,1174	-0,4595	0,2248	-0,5353	0,2745	-0,6129	0,3264	-0,6907	0,3791
1,8mm CF/PEEK	-0,3193	0,1541	-0,5308	0,2726	-0,1434	0,1274	-0,1732	0,1610	-0,2041	0,1950
2mm SS	-0,2915	0,1363	-0,3262	0,1461	-0,3613	0,1626	-0,3972	0,1822	-0,4310	0,2015
2mm Ti	-0,3887	0,1761	-0,4632	0,2201	-0,5389	0,2689	-0,6165	0,3204	-0,6951	0,3727
2mm CF/PEEK	-0,4393	0,2063	-0,5350	0,2670	-0,6329	0,3329	-0,1760	0,1573	-0,2079	0,1903

By monitoring the safety factor of the rings, it can be concluded that stainless steel rings are deformed permanently under higher pretension loads. This permanent

deformation occurs for 1100 N and 1300 N 1.8 mm k-wire tension for the 2 mm k-wires stainless steel ring are further deformed under 1300 N of tension load. On the other hand CF/PEEK rings appear to have increased safety factor (more than 15) and therefore Ansys is impossible to show the exact value. The values of minimum safety factor of the rings is shown in Table XVII and Figure 33.

Table XVII Ring minimum safety factor during second load step

	BOLT PRETENSION (N)				
FRAME	**500**	**700**	**900**	**1100**	**1300**
1,8 mm SS	1,9026	1,4164	1,0651	0,84986	0,70584
1,8 mm Ti	8,2539	5,7811	4,2862	3,096	2,4429
1,8 mm CF/PEEK	15	15	15	13,499	10,596
2 mm SS	2,49	1,7784	1,3778	1,1201	0,93592
2 mm Ti	11,194	7,7291	5,5959	4,3457	3,5009
2 mm CF/PEEK	15	15	15	15	15

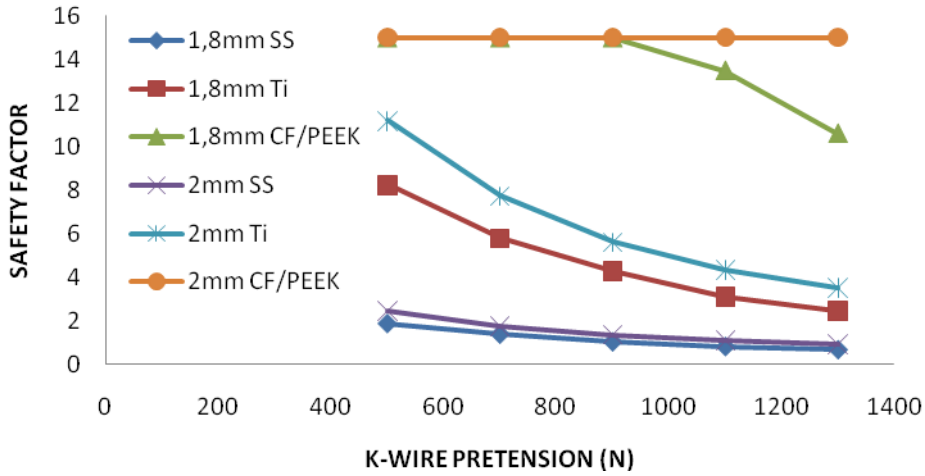

Figure 33 Minimum safety factor of the ring assembly

Safety factor minimum values have also been monitored for the k-wire, showing stainless steel wire permanent deformation even in low k-wire tension loads, which is a result of the k-wires being in the non-linear material zone even from the first load step. The minimum values of the k-wire safety factor are shown in Table XVIII.

Table XVIII Minimum safety factor of the k-wire during second load step

	BOLT PRETENSION (N)				
FRAME	**500**	**700**	**900**	**1100**	**1300**
1,8mm SS	0,82869	0,5603	0,4384	0,35825	0,30105
1,8mm Ti	3,5371	2,5161	1,9205	1,5458	1,2899
1,8mm CF/PEEK	3,9347	2,7481	2,1161	1,715	1,4425
2mm SS	0,92937	0,67703	0,52992	0,4355	0,36656
2mm Ti	4,3052	3,0647	2,347	1,89	1,5743
2mm CF/PEEK	6,0331	4,1934	3,2124	2,6115	2,1963

Minimum safety factor reduction on the k-wires is clearly shown in Figure 34. This figure shows the difference between minimum safety factor values for k-wires of the same material with different diameter. This difference is increasing as the modulus of elasticity of the material decreases.

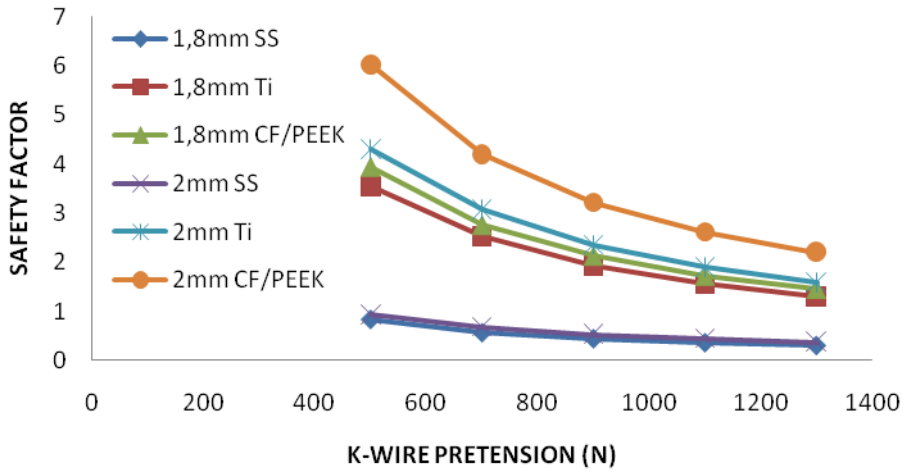

Figure 34 Minimum safety factor of the k-wires during second load step

Stress concentration at the bone due to the dead load application can be seen in Table XIX. Maximum von Mises stress is increasing as the tension of the wires increases. It also appears to be increased to k-wires of the same diameter because of the modulus of elasticity of the different materials

Table XIX Equivalent stress on femur during second load step

	BOLT PRETENSION (N)				
FRAME	**500**	**700**	**900**	**1100**	**1300**
1,8mm SS	19,762	29,248	38,468	47,766	57,097
1,8mm Ti	49,834	71,408	92,798	114,39	135,92
1,8mm CF/PEEK	52,609	75,325	97,822	120,7	143,5
2mm SS	15,681	18,75	24,886	31,023	37,314
2mm Ti	32,532	46,798	61,097	75,276	89,497
2mm CF/PEEK	34,311	49,363	64,437	79,263	94,249

Comparing the femur equivalent stress maximum values of the second load step shown in Figure 35 to those of the first load step shown in Figure 28, an increase of the stresses is observed with the increase of the k-wire pretension, but these stress values of the two load states are similar for the different configurations .

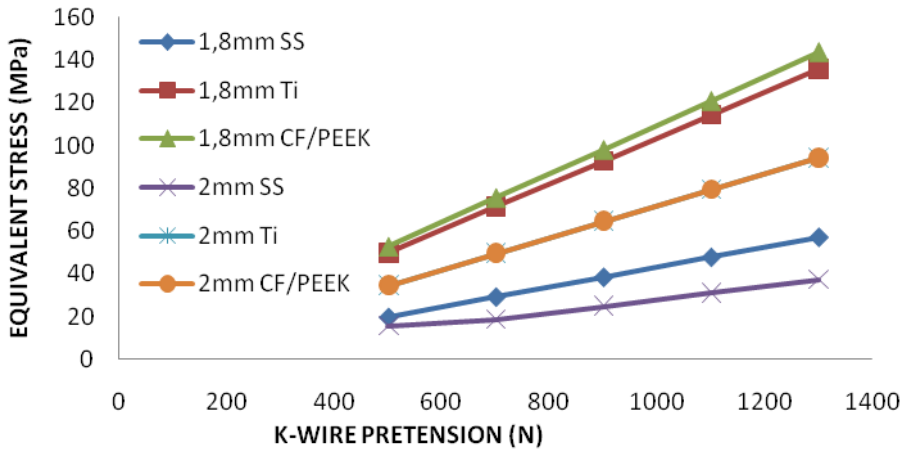

Figure 35 Equivalent stress on femur during second load step

The fragment area displacement shown in Table XX appears to be decreased as the k-wire tension increases. This decrement is also mentioned by A. Georgadakis (2010), even though it appears to be significantly smaller in the present study because of important differences in the 3D modeling of the fragment area. The differences between the studied configurations of the frame though seem to be negligible. Therefore, the graph of Figure 36 will help for the better understanding of the reduction rate.

Table XX Fragment area total deformation during second load step

	BOLT PRETENSION (N)				
FRAME	**500**	**700**	**900**	**1100**	**1300**
1,8mm SS	0,1039	0,1015	0,1010	0,1006	0,1001
1,8mm Ti	0,1034	0,1015	0,1010	0,1007	0,1009
1,8mm CF/PEEK	0,1034	0,1018	0,1014	0,1013	0,1020
2mm SS	0,1015	0,1010	0,1005	0,1001	0,0993
2mm Ti	0,1018	0,1012	0,1007	0,1004	0,1002
2mm CF/PEEK	0,1020	0,1015	0,1012	0,1010	0,1014

The calculated displacement of the fragment area shown in Table XX appears to be equal to 10% of the daily distraction of the femur and therefore this amount of displacement will stimulate the osteogenesis process according to M.A. Gatani (2011). The percentage though or the absolute value of the allowable fragment area displacement needs further studies to be established. The reduction rate of the fragment area displacement for the different configurations of the frame is shown in Figure 36.

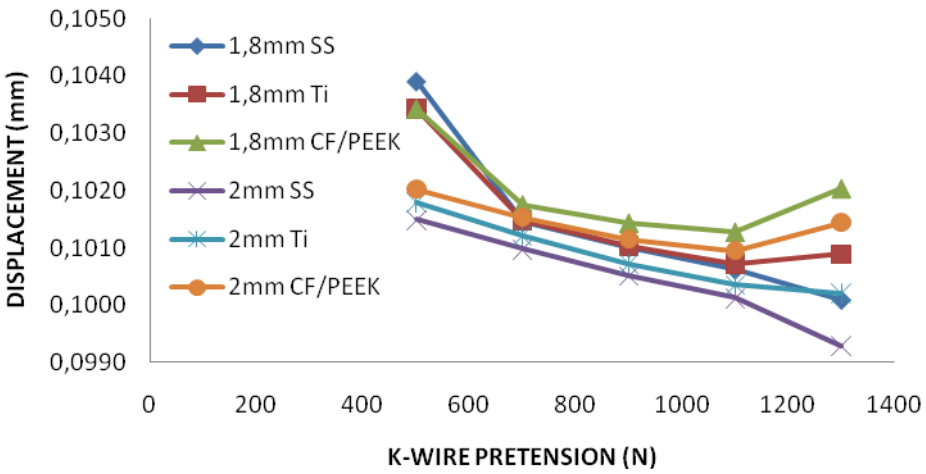

Figure 36 Fragment area total deformation during second load step

Typical equivalent stress distribution for the 1.8 Ti-6Al-4V k-wires along their axis is shown in Figure 38. The results illustrate the differences in stress distribution of the same wire for the different pretension loads. Higher stresses are observed for higher values of pretension. The maximum value is located close to the wire ends, at the points where the wire is leaving the clamping bolt. Close to the center of the wire, two small decrements of the stress value are visible. These stress perturbation regions correspond to the insertion points of the wires in both directions and the lower values represent the wire-bone interfaces. The contact between k-wires and the femur results in lower stress values at the area of the contact.

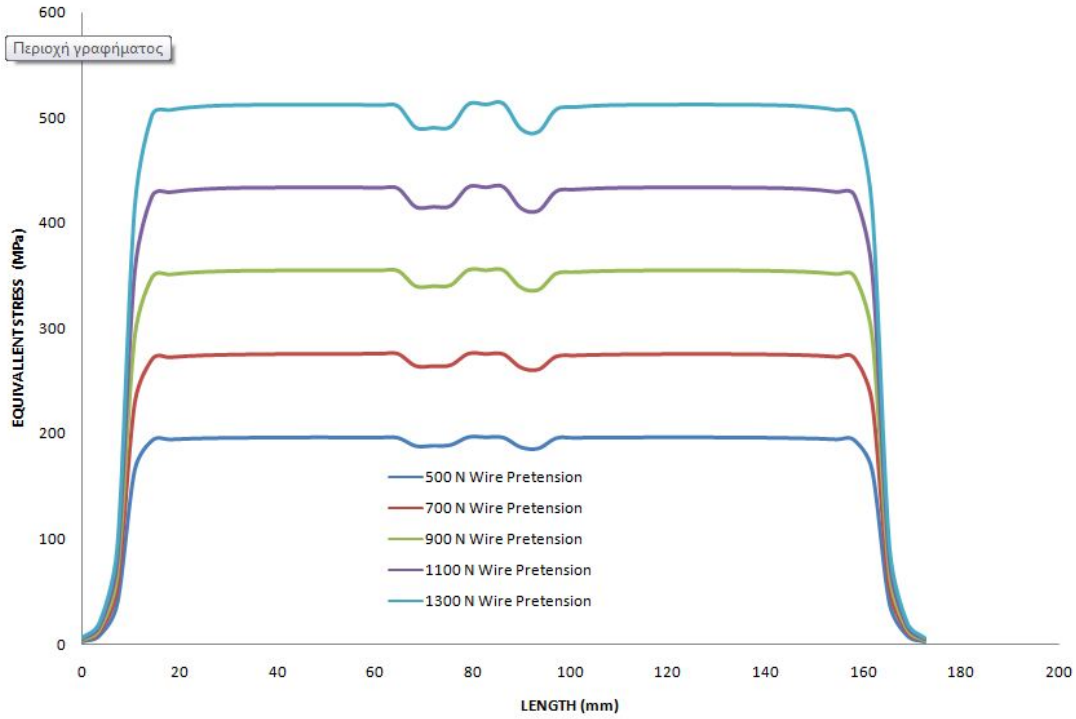

Figure 37 Equivalent stress distribution on Ti-6Al-4V k-wires.

Figure 38 shows the typical stress distribution, along 1.8 mm k-wires of the studied materials. Even though the stress maximum values for the stainless steel and titanium alloy are at the same location there are differences in the stress values the k-wire-bone interfaces. The curves also reveal that at the contact areas the materials with lower modulus of elasticity tend to develop lower stress values with the femur. Additionally, as shown in the case of the CF/Peek material, the overall stress distribution along the k-wire is significantly lower due to the lower Young's modulus of this material.

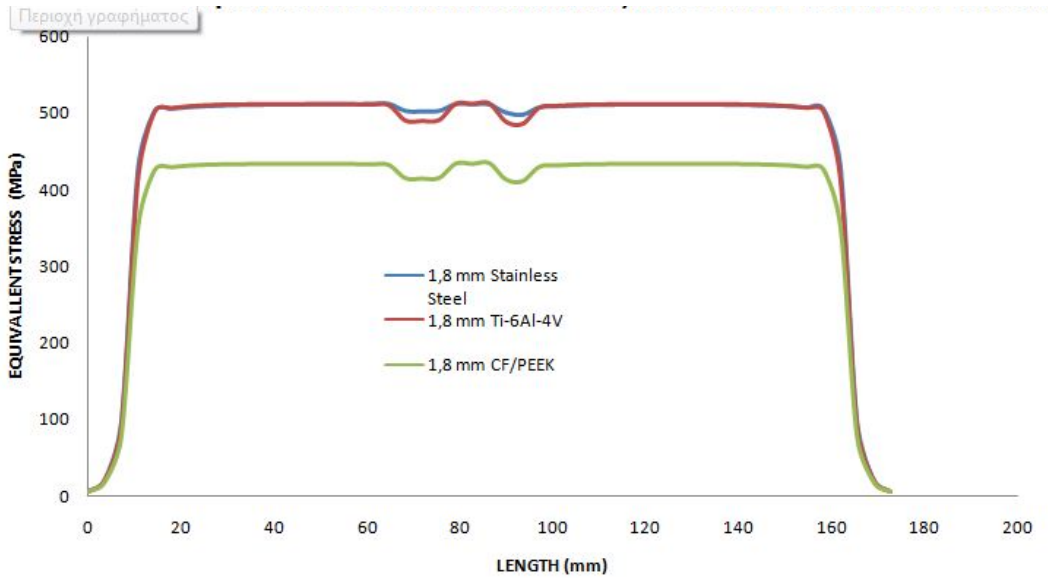

Figure 38 Equivalent stress distribution in 1.8mm k-wires

Equivalent stress distribution in 1.8 mm and 2 mm stainless steel k-wires tensioned at 1300 N are shown in Figure 39. Even though the material is the same, difference in the maximum equivalent stress value and location are visible. The difference in

diameter results to lower equivalent stress value for the 2 mm k-wire. The local maximum equivalent stress is located at the insertion point of the k-wire to the bone because of different stress distribution.

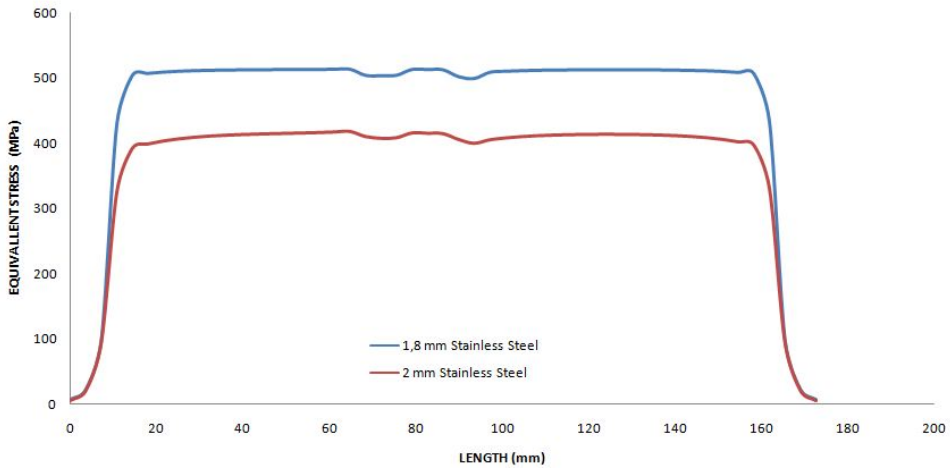

Figure 39 Equivalent stress distribution in stainless steel k-wires tensioned at 1300N

The results of the equivalent stress distribution are in agreement with T.N. Board (2007) study for the pressure distribution at the wire bone interface. Equivalent stress reaches a uniform level approximately 10 mm from clamping bolts. Stress is rising in relation to the tension load as observed in Figure 37. The decrement of equivalent stress at the contact area indicates that the force is being absorbed at these areas of the k-wire/femur interface.

5. Conclusions

From the conducted research it can be concluded that the material rigidity of the ring assembly is very important for the stiffness of the apparatus. Stiffer materials tend to deform less resulting in smaller stress values to the bone because of the k-wire tension. Stainless steel wires also perform better and they are more orthopedically acceptable regarding the bone load.

Ti-6Al-4V alloy appears to be more suitable for the k-wires, since it is not deforming permanently resulting in a more stable environment for the osteogenesis process. Though, the rings have to be more rigid concerning the bending loads. In order to reduce their deformation under k-wire tension a further redesign of the rings is necessary.

CF/PEEK composite may perform better than the rest of the studied materials in the k-wires but the increased deformation values under tensioned wires is eliminating this advantage. Redesign of the rings is necessary along with the rearrangement of the reinforcement phase to achieve greater stiffness.

6. Future Work

The performance of the studied materials, should be investigated further by reducing the variables of this study. Safer results could be extracted by the use of stainless steel k-wires and combine them with k-wires of the other studied materials. By this approach the displacement of the k-wires, because of the ring's deformation, will not be a determinant factor for the k-wire-bone interface and the effect of the different materials on bone damage will be elucidated.

Redesign of the Ilizarov external bone fixator with CF/PEEK needs to be made, with respect to the proper arrangement of the reinforcement phase, in order to achieve the desired stiffness of the rings and the ideal performance of the apparatus. Such a design will allow the physicians to obtain X-rays during the postoperative process and have a clear picture of the bone location during the distraction phase and achieve better alignment in complicate cases.

References

- A. Georgadakis (2010) Biomechanical analysis of the Ilizarov external bone fracture fixation system, Thessaly University
- A.J.S. Renard, B.G. Schutte, N. Verdoschot, A Van Kampen (2005) The Ilizarov external fixator: What remains of the wire pretension after dynamic loading, The Netherlands
- A. R. Zamani, S. O. Oyadiji (2010) Theoretical and Finite Element Modeling of Fine K-wires in Ilizarov External Fixator, ASME
- A.W. Davidson, M. Mullins, D. Goodier, M. Bary (2003) Ilizarov wire tensioning and holding methods: a biomechanical study, United Kingdom
- A. Yanez, J.A. carta, G. Garces (2010) Biomechanical evaluation of a new system to improve screw fixation in osteoporotic bones, Gran Canaria Spain
- B.Ji, G. Jiang, J. Long, H. Wang (2010) Why high frequency if distraction improved the bone formation in distraction osteogenesis, Chengdu China
- B. Narayan,D.R. Marsh (2003) The Ilizarov method in the treatment of fresh fractures, United Kingdom
- C. Migliaresi, F. Nicoli, S. Rossi, A. Pegoretti (2004) Novel uses of carbon composites for the fabrication of external fixators, Italy
- C. Khodadadyan, M. Raschke, T. Mittlemeier, I. Melcher, N.P. Haas (2001) Ankle and pan-talar arthrodesis with ilizarov composite hybrid fixation: operative technique and review of 21 cases, Berlin
- D. Haines (2000) My Ilizarov experience, United Kingdom
- E. Antonova*, T Kim Le, R. Burge and J. Mershon (2013) Tibia shaft fractures: costly burden of non unions, Indianapolis USA).
- E.L. Steinberg, E. Rath, A. Shlaifer, O. Chechik, E. Maman, M. Salai (2013) Carbon fiber reinforced PEEK Optima - A composite material biomechanical properties and wear/debris characteristics of the CF-PEEK composites for orthopedic trauma implants, Israel
- E. Yilmaz, O. Belhan, l. Karakurt, N. Aslan, E. Serin (2003) Mechanical performance of hybrid Ilizarov external fixator in comparison with Ilizarov circlular external fixator, Elazig Turkey

- F.Tanaka, T. Okabe, H. Okuda, I.A. Kinloch, R.J. Young (2013) Factors controlling the strength of carbon fibers in tension
- G.N. Duda, F. Mandruzzato, M. Heller, J.P. Kassi, C. Khodadadyan, N.P. Haas (2002) Mechanical conditions in the internal stabilization of proximal tibial defects, Berlin Germany
- H. Luo, G. Xiong, Z. Yang, S.R. Raman, Q. Li, C. Ma, D. Li, Z. Wang, Y. Wan (2014) Preperation of three- dimensional braided carbon fiber-reinforced PEEK composites for potential load bearing bone fixations. Part I. Mechanical properties and cytocompatibility.
- H. Stein, R. Morsheiff, F. Baumgart, S.M. Perren, J. Cordey (1997) The hybrid ring tubular external fixator: a biomechanical study
- J.A.Alierta, M.A. Perez, J.M. Garcia-Aznar (2013) An Interface Finite Element Model can be used to predict healing outcome of bone fractures, Spain
- J. Gessmann, B. Jettkant, M. Konigshausen, T. Armin Schildhauer, D. Seybold (2012) Improved wire stiffness with modified connection bolts in Ilizarov external frames; a biomechanical study, Bochum Germany
- J. Gessman, B. Jettkant, T. Armin Schildhauer, D. Seybold (2011) mechanical stress on tensioned wires at direct and indirect loading: A biomechanical study on the Ilizarov external fixator, Bochum Germany
- J. Lammens, M. Van Laer, R. Motmans (2007) Ilizarov treatment for femoral mal-union or non union associated with fatigue fracture of an intramedullary nail, Belgium
- J. Zhang, S. Ju, D. Jiang, H.X. Peng (2013) Reducing dispersity of mechanical properties of carbon fiber/epoxy compositesby introducing multiwalled carbon nanotubes.
- K.D. Bouzakis, S. Mitsi, N. Michailidis, I. Mirisidis, G. Mesomeris, G. Maliaris, A. Korlos, G. Kapetanos, P. Antonarakos, K. Anagnostidis (2004) Loading Simulation of lumpar spine vertebrae during a compression test using the finite element method and trabecular bone strength properties, determined by means of nanoindentations, Aristotle University of Thessaloniki

- K. Fujihara, Z.M. Huang, S. Ramakrishna, K. Satkanantham, H. Hamada, (2004) Feasibility of knitted carbon/ PEEK composites for orthopedic bone plates.
- K. Karunratanakul, J. Schrooten, H. Van Oosterwyck (2010) Finite element modeling of a unilateral fixator for bone reconstruction: Importance of contact settings, Belgium.
- K.L. Baker, M. Burns, S. Littler (1999) Physiotherapy for patients with an external fixator
- L.C. Rogers, N.J. Bevilacqua, R.G.Frykberg, D.G. Armstrong (2007) Predictors of postoperative complications of Ilizarov external ring fixator in the foot and ankle
- L. Lewandowski, S.M. Tintle, C. Daniel, J.A.O'Daniel, M. fleming, J. Keeling (2013) Circular external fixator for treatment of distal humerus fractures: Case report, USA
- L. N. Solomin, (2005) The Basic Principles of External Fixation Using the Ilizarov Device "MorsarAV", Saint Petersburg.
- M.A. Catagni, F. Guerreschi, L. Lovisetti (2011) Distraction osteogenesis for bone repair in the 21st century: Lessons learned, Italy
- M.G. Lee, K Chung, C.J. Lee, J.H. park, J. kim, T.J. kang, J.R. Youn (2001) The viscoelastic bending stiffness of fiber reinforced compocite illizarov rings, South Korea
- M.M. Mullins, A.W. Davidson, D. Goodier, M. Barry (2003) The biomechanics of wire fixation in the Ilizarov system, United kingdom
- M. Mrazek, Z. Florian, R. Vesely, L. Borak,(2010) Strain-stress analysis of lower limb with applied fixator, University of west Bohemia
- M. Pitkin, Y. Shukeylo, A. Gritsanov (2007) Mathematical modeling of fixation of a bone fragment in a new Double-needle external Fixator compared to hoffmann ii fixator.
- M. Tyllianakis, S. Mylonas, A. Saridis, A. Kallivokas, A. Kouzelis, P. Megas (2009) Treatment of unstable distal radius fracture with illizarov circular, nonbridging external fixator, University of Patras

- N.A. Osei, B.M. Bradley, P. Culpan, J.B. Mitchell, M. Bary, K.E. Tanner (2006) relationship between locking-bolt pretension in the Ilizarov frame, United Kingdom
- N.Bor, G. Rubin, N.Rozen (2011) ilizarov method for gradual deformity correction.
- O. Baran, H. Havitcioglu, H. Tatari, B.Cecen (2008) The stiffness characteristics of hybrid Ilizarov fixators, Izmir Turkey
- P. Fenton, j. Phillips, S. Royston (2006) The use of illizarov frames in the treatment of pathological fracture of the femur secondary to osteomyelitis A review of three cases, United Kingdom
- P.J. Hillard, A.J. Harrison, R.M. Atkins (1998) The yielding of tensioned fine wires in the Ilizarov frame, Proc. Inst. Mech. Eng. [H] 212,37-47
- P. Krisnhakanth (2012) Mechanical Considerations In Fracture Fixation, Queensland University of Technology.
- P. Megas, A. Saridis, A. Kouzelis, A. Kallivokas, S, Mylonas, M. Tyllianakis (2010) The treatment of infected non union of the tibia following intramedullary nailing by the Ilizarov method, University of Patras
- R.A. Raimondo, D.L. Skaggs, M.P.Rosenwasser, H,M, Dick (1999) Lengthening of pediatric forearm deformities using the Ilizarov technique: Functional and cosmetic results, New York
- R. Littlewood (2007) The Benefits and Risks of the Ilizarov Technique for Limp Reconstruction, Paris University
- S. A. Green (1989) Ilizarov orthopedic methods, USA
- S. Britten, A. Ghoz, B. Duffield, P. Giannoudis (2013) Ilizarov fixator pin site care: the role of crusts in the prevention of infection, Leeds United kingdom
- S.H Ralston (2013) Bone structure and metabolism.
- S.Ramakrishna, J. Mayer, E. Wintermantel,K.W. Leong (2001) Biomedical applications of polymer composite materials: a review
- S. Simard, M. Marchant and G. Mencio (2013) The Ilizarov Procedure: Limb Lengthening and Its Implications, http://ptjournal.apta.org/ 2013

- T.N. Board, L. Yang, M. Saleh (2007) Why fine wire fixators work: An analysis of pressure distribution at the wire-bone interface, United Kingdom
- T. Zigman, S. Davila, I. Dobric, T. Antoljak, G. Augustin, D. Rajacic, T. Kovac, T. Ehrenfreund (2013) Intraoperative measurement of bone electrical potential: a piece in a puzzle of understanding fracture healing, Zagreb Croatia
- V. La Russa, B. Skallerud, J. Klaksvik, O. Foss (2010) Wire tension versus wire frequency: An experimental Ilizarov frame study, Trondheim Norway
- V. La Russa, B. Skallerud, J. Klaksvik, O. Foss (2011) Reduction in wire tension caused by dynamic loading. An experimental Ilizarov frame study, Trondheim Norway
- W. Walke, J. Marciniak, Z. Pasxenda, M. Kaczmarek (2008) Biomechanical analysis of tibia - double threaded screw fixation.